This is a pre print version of the following article:

Analog and digital worlds: Part 2. Fourier analysis in signals and data treatment / Seeber, Renato; Ulrici, Alessandro. - In: CHEMTEXTS. - ISSN 2199-3793. - 3:2(2017), pp. 1-15. [10.1007/s40828-017-0044-x]

Terms of use:

The terms and conditions for the reuse of this version of the manuscript are specified in the publishing policy. For all terms of use and more information see the publisher's website.

10/10/2024 06:15

(Article begins on next page)

ChemTexts

Analog and digital worlds: Part 2. Fourier analysis in signals and data treatment

--Manuscript Draft--

Manuscript Number:	
Full Title:	Analog and digital worlds: Part 2. Fourier analysis in signals and data treatment
Article Type:	Lecture Text
Funding Information:	
Abstract:	The most direct scope of Fourier Transform (FT) is to give an alternative representation of a signal: from the original domain (time-domain or space-domain or whatever independent-variable-domain) to the corresponding frequency domain. This subject has been dealt with in Part 1 [1] In particular, the 'Fourier-transformed' signal, or simply 'spectrum' of the signal, has been exploited to calculate the lowest sampling frequency suitable to achieve a correct representation of the signal itself. In a section of the present contribution, it is illustrated how a process called windowing allows the application of FT to periodic sequences: proper preliminary truncation, i.e., isolation of a finite portion of the signal, is necessary. The meaning of the convolution and deconvolution operations is also discussed. It is shown how, through the convolution theorem, FT allows a very effective alternative path to the execution of these operations in the original domain. Examples are given of manipulation, through deconvolution, of experimentally measured signals that arise as a result of the 'spontaneous' convolution of two concurrent events, in order to isolate the responses ascribable to the single events.
Corresponding Author:	Renato Seeber, Professor Department of Chemical and Geologival Sciences University of Modena and Reggio Emilia Modena, MO ITALY
Corresponding Author Secondary Information:	
Corresponding Author's Institution:	Department of Chemical and Geologival Sciences University of Modena and Reggio Emilia
Corresponding Author's Secondary Institution:	
First Author:	Renato Seeber, Professor
First Author Secondary Information:	
Order of Authors:	Renato Seeber, Professor
	Alessandro Ulrici, Associate Professor
Order of Authors Secondary Information:	
Author Comments:	Sorry: I don't manage to add Stephen Fletcher to the suggested reviewrs: Stephen.Fletcher@lboro.ac.uk He's well known to be among the most expert scientist in the field
Suggested Reviewers:	Alvaro Colina, Associate Professor Universidad de Burgos acolina@ubu.es Expert in treatment of experimental data and signals

Powered by Editorial Manager® and ProduXion Manager® from Aries Systems Corporation

Manuscript Click here to download Manuscript FT_Part_2.docx

Analog and digital worlds: Part 2. Fourier analysis in signals and data treatment

Renato Seeber[1] • Alessandro Ulrici[2]

[1] Renato Seeber (✉)
Department of Chemical and Geological Sciences
Via G.Campi, 103
41125 Modena (Italy)
email: renato.seeber@unimore.it

[2] Alessandro Ulrici
Department of Life Sciences
Padiglione Besta, Via Amendola, 2
42122 Reggio Emila (Italy)

Keywords: *windowing, filtering, convolution and deconvolution, Fourier analysis*

Abstract The most direct scope of *Fourier Transform* (FT) is to give an alternative representation of a signal: from the original domain (time-domain or space-domain or whatever independent-variable-domain) to the corresponding frequency domain. This subject has been dealt with in Part 1 [1] In particular, the 'Fourier-transformed' signal, or simply 'spectrum' of the signal, has been exploited to calculate the lowest sampling frequency suitable to achieve a correct representation of the signal itself. In a section of the present contribution, it is illustrated how a process called *windowing* allows the application of FT to periodic sequences: proper preliminary *truncation*, i.e., isolation of a finite portion of the signal, is necessary. The meaning of the *convolution* and *deconvolution* operations is also discussed. It is shown how, through the *convolution theorem*, FT allows a very effective alternative path to the execution of these operations in the original domain. Examples are given of manipulation, through deconvolution, of experimentally measured signals that arise as a result of the 'spontaneous' convolution of two concurrent events, in order to isolate the responses ascribable to the single events.

Introduction

In Part 1 of this series [1] we dealt with quite a diffused mathematic tool: *Fourier Transform* (FT or DFT for *Discrete Fourier Transform*, when applied to a numerical sequence of data, rather than to a function) [2-9]. DFT constitutes an algorithm of fundamental importance in the treatment of signals and data. However, in the common practice, the computational details, as well as the operations exploiting DFT, are most often 'transparent to the user', being directly executed by the software managing an instrument. As a result, the operator could ignore the way how the final instrumental response is obtained: DFT is at the basis of modern spectroscopic techniques like infrared (FT-IR), microwave and nuclear magnetic resonance (FT-NMR) spectroscopies, but also of faradic impedance, mass spectrometry (Ion Cyclotron Resonance Spectroscopy [6]), and other instrumental methods [6,7].

It is evident that, in the case of FT-based instrumentation, little or even no expertise at all is requested to the user to obtain the output signal. However, aiming at the most suitable treatment of data and signals of different nature, a completely 'passive' approach does not always constitute the best choice. In Ref. [1] we dealt with more or less trivial examples of *original signals* that are transformed by means of FT into the corresponding *spectra*, leading to an equivalent representation in the frequency domain. It often happens that such a transformation into a spectrum is the best (or even the only) way to obtain useful information, i.e., to interpret the data collected in chemical terms.

Furthermore, as to elaboration of signals or data sets, the execution of a number of operations on the relevant spectra results definitely more simple in comparison to the equivalent calculations executed directly on the original responses. This is the case of operations described in the present article, such as *convolution* and *deconvolution*. In particular, performing deconvolution of signals in the original domain may require long times and high computational loads, while, by using FT, this operation is much faster and easier to be accomplished.

When manipulating signals, the term convolution is often used as a synonym of *signal filtering*, or *digital signal filtering* [2,3,5,9]. It is a branch of science that was born in the frame of electronics and is nowadays a very important issue in all experimental sciences. For chemists, the meaning of signal filtering is often restricted to the *low-pass filtering* operation, which means removal of the high frequency content of the signal. However, filtering can be also used to perform many other operations, ranging from the simplest ones, such as differentiation, to more complex elaborations.

On the one hand, convolution and deconvolution operations may be intentionally performed to achieve a variety of goals; on the other hand, they are also often 'hidden' within a signal that results from 'mixing' of different physical phenomena. In principle, whenever mixing occurs through convolution, deconvolution is the mathematical operation that may separate the individual contributions to the overall signal. It is evident that the analysis of the effects of the individual components may lead back to the identification of the characteristics of the corresponding individual sources.

FT algorithm operates on a finite number of data, i.e., on finite sequences. When an infinite length signal is submitted to Fourier transformation, it must be therefore properly truncated, i.e., sectioned. However, FT implicitly ascribes periodic character to the signal that is analysed: the isolated segment is viewed as the period of a sequence, not necessarily coincident with that of the original signal, as depicted in Fig. 1. The procedures to properly truncate the whole original sequence (*windowing*) constitute therefore the beginning of the present contribution.

In this respect, it is worth noticing that this Part 2 should be considered as the prosecution of Part 1 [1]. For this reason, arguments already discussed there will be considered as if they were treated here, in preceding pages. This also holds for the meaning of some symbols.

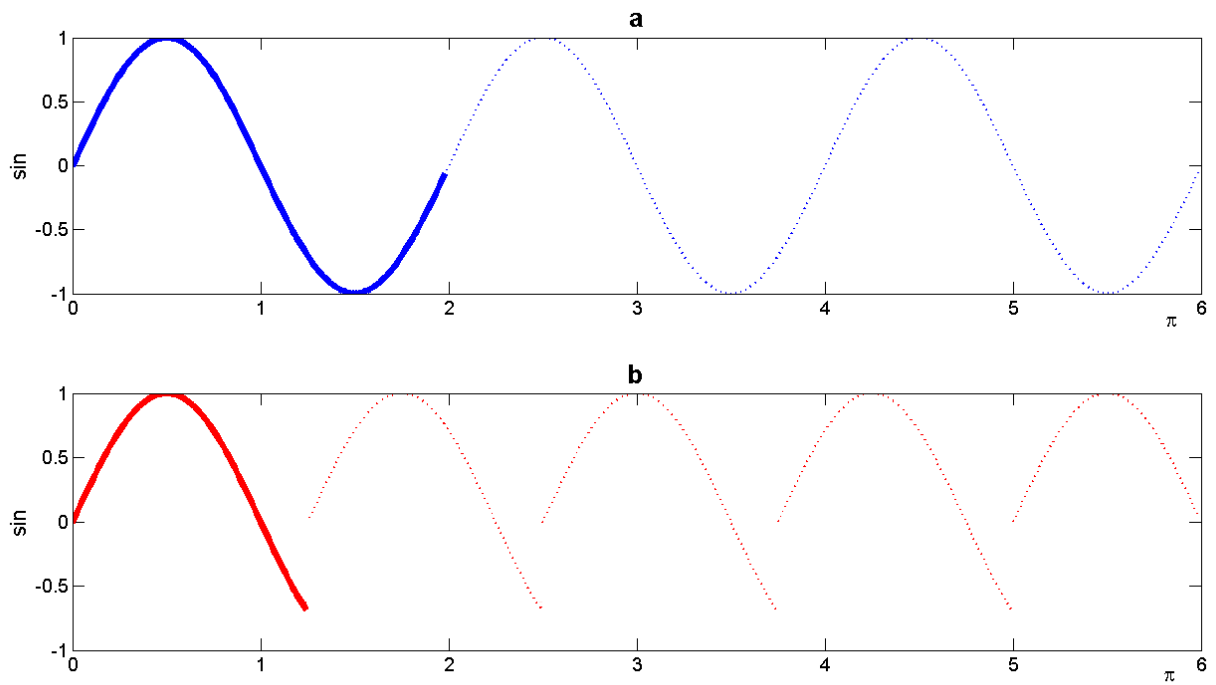

Fig. 1 (a) A single period accounts for the whole periodic sequence; (b) a fraction of one single period does not.

Windowing

In Ref. [1] we have dealt with a periodic signal of infinite length, as expressed by the function $f(t)$ and by the equivalent sequence $y(k)$; the corresponding fitting function $g(t)$ and fitting sequence $x(k)$ are defined. For short, whenever possible, y and x are used instead of $y(k)$ and $x(k)$, respectively, from here onwards.

In order to consider a finite number of points that are representative of the whole signal, it is necessary to truncate it, i.e., to look at it through a *window*: windowing is necessary in order to deal with a finite length sequence, consisting of a finite number of points, N.

Actually, the finite sequences which are most often encountered in chemistry, where the phenomena are most often of finite length, should be considered in the same way as the results of a proper truncation of periodic signals

In the frame of FT, considering cosines and sines as the set of basis functions [1], Eq. (1) [Eq. (15) in Ref. [1]] expresses the periodic character of the result of the transformation (as anticipated, see Ref. [1] for the meaning of symbols):

$$x(k) = \sum_{h=0}^{N/2} \left[A_h \cos\frac{2\pi hk}{N} + B_h \sin\frac{2\pi hk}{N} \right] \qquad (1)$$

As it was discussed in Ref [1], to many purposes, such as to perform simple filtering operations[a], it is sufficient to consider the modulus of the spectrum of x, which is generally referred to as the *magnitude spectrum*:

$$M_h = \sqrt{(A_h^2 + B_h^2)} \qquad (2)$$

[a] In the forthcoming discussion, we will be focused on the modulus of the frequencies contained in the spectrum, more than on their phase. To this aim, the use of the magnitude spectrum, as defined in Eq. (2), is therefore enough, since it accounts for the weight of each frequency in the spectrum. The phase spectrum describes instead the 'delay' in the original domain of each one of the h frequency components, which depends on the ratio between the corresponding A_h and B_h coefficients, and is defined as $\vartheta_h = \text{artctan}(B_h/A_h)$. By considering two different signals with the same magnitude spectrum but with different phase spectra, they will not appear identical in the time domain. Therefore, magnitude spectrum and phase spectrum are independent from each other, since they account for different aspects of the signal, and are both necessary to reconstruct the sequence through inverse Fourier Transform. This also holds whenever the frequencies are submitted to filtering operation, where the phase spectrum is untouched.

As it was anticipated in the Introduction section, when dealing with a finite sequence, this is considered by DFT as the single period of a periodic sequence, repeated an infinite number of times. Fig. 2a reports the points obtained by sampling and truncating a cosine function to generate a (finite) sequence: the length of the window, i.e., of the truncation interval, is an integer multiple of the cosine period, so that the plot of the vector modulus *vs*. frequency only exhibits one component with amplitude different from 0 (Fig. 2b). On the basis of the spectrum in Fig. 2b,and of the corresponding plot of phase *vs*. frequency, the cosine periodic sequence in Fig. 2a is reconstructed.

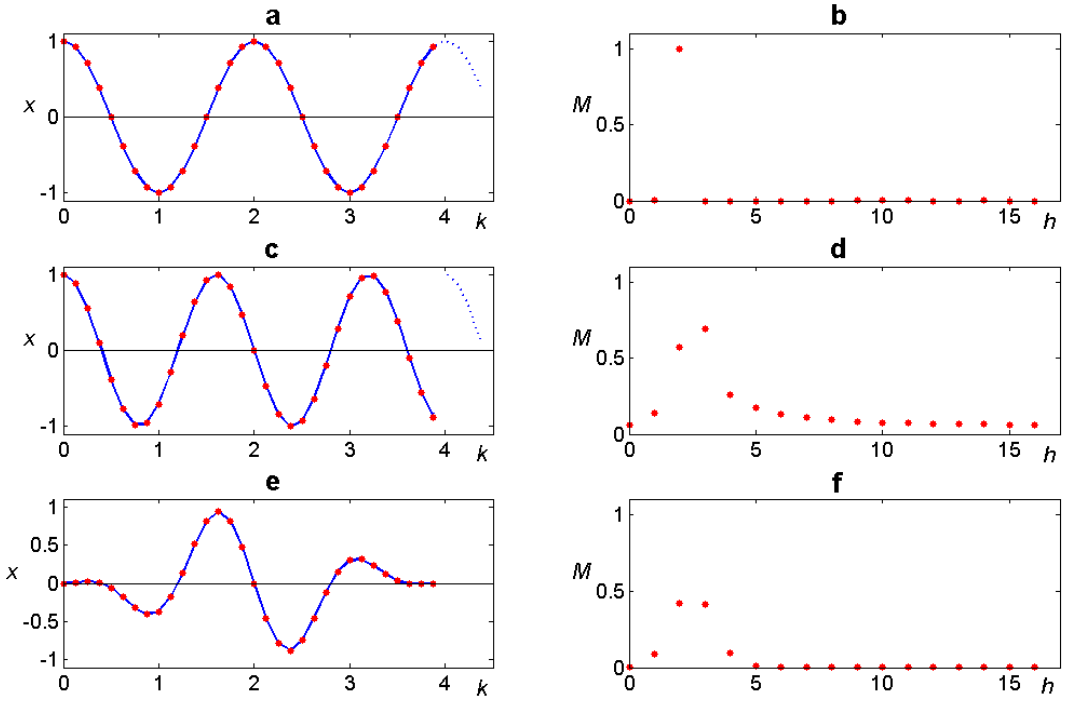

Fig. 2 In (a) and (c) two cosine sequences obtained by truncation with a boxcar (see Fig 3a); (e) cosine sequence obtained by truncation with a Hanning window (Fig. 3c). In (b), (d) and (e) the magnitude spectra obtained from (a), (b) and (c), respectively , are reported.

In the windowing operation outlined in Fig. 2a the weight attributed to the points that are selected on the cosine function is either 1 (points within the window) or 0 (points outside the window), according to what accounted for by the so-called *rectangular window*, reported in Fig. 3a. Since the truncation interval is a multiple of a period of the windowed cosine, the obtained spectrum (Fig. 2b) accounts for the original periodic function, which is correctly reconstructed.

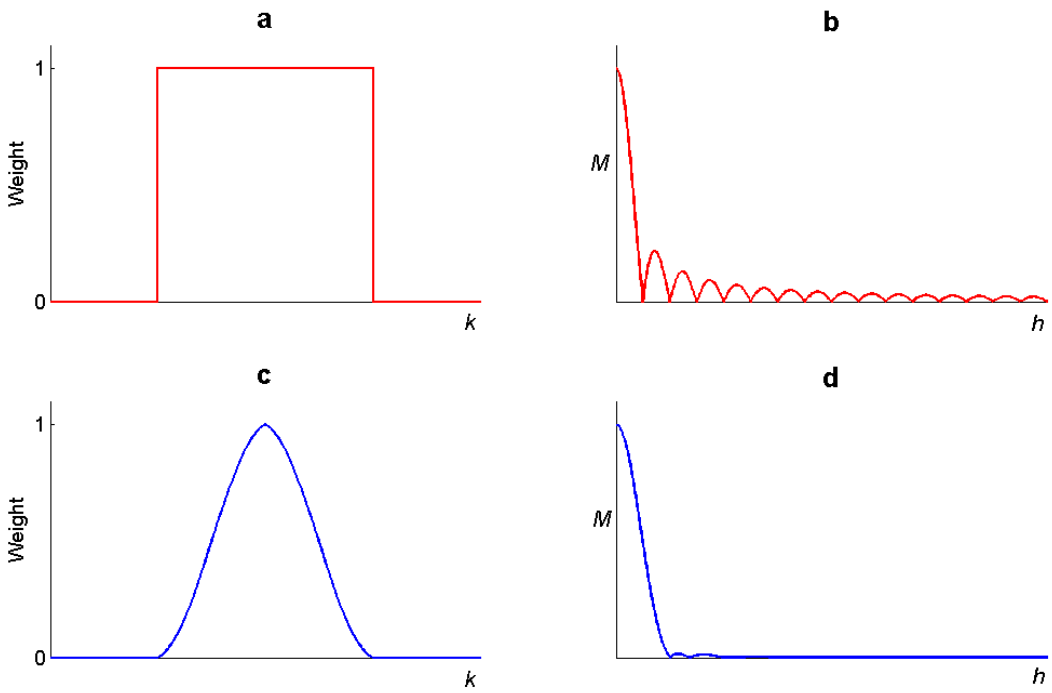

Fig. 3 (a) Rectangular window and (b) relevant magnitude spectrum; (c) Hanning window and (d) relevant magnitude spectrum.

On the other hand, the windowed interval in Fig. 2c, where the rectangular window in Fig. 3a is once more used, is not an integer multiple of the cosine period. As a result, in Fig. 2d more or less high values are found for the amplitudes of any frequencies of the spectrum: spurious frequencies arise. Such an undesired effect is called *spectral leakage*: a periodic function different from a cosine is actually processed by the DFT operation. There is, in fact, a sharp discontinuity at the extremes of two adjacent periods: the spectrum computed by DFT should account for a periodic function in which similar sharp discontinuities are present. As a consequence, high frequencies should be part of the spectrum. The reconstructed signal exhibits spurious oscillations in the proximity of the discontinuity: they are ascribed to the so-called *Gibbs phenomenon* [b]. Gibbs phenomenon may be reduced by using a window suitable to smooth the discontinuities at the beginning and end of the truncated sequence: such a window performs effective *apodization*[c]. Reduction of the amplitudes of the *spurious frequency components* may be realised by properly weighting the points of the truncated sequence. Windows doing this most often represent preferable alternatives to the rectangular window in Fig. 3a; as an example, Fig. 2e shows a cosine

[b] The Gibbs phenomenon arises from the inherent difficulty in approximating a discontinuity by a finite number of sines and cosines. The example of a square wave is reported in the following.

[c] Recalling the etymology of the word, the term is self-explanatory: removing the foot (from the Greek word podos – ποδός).

function truncated in the same way as in Fig. 1c, in which, however, each point of the resulting sequence is weighted by the *Hanning window* (see Fig. 3c): the leakage is strongly reduced. The resulting spectrum, reported in Fig. 2f, better accounts for frequencies that 'do count' in the description of the original signal, i.e., those closest to the only frequency present in Fig. 2b. Much lower values are instead assumed by spurious frequencies, with respect to Fig. 2d. As it will be shown in the following sections, this is strictly related to the shape of the spectra of the rectangular window and of the Hanning window, reported in Fig. 3b and in Fig 3d, respectively.

Summarising, Fig. 3 shows two different windows through which to look at the original signal: a rough *rectangular window* (Fig. 3a), which has been invoked for truncation of the sequences in Fig. 2a and 2c, and a *Hanning window* (Fig. 3c). In Fig. 3b and in Fig. 3d the spectra corresponding to the two windows are shown. The presence of spurious oscillations, more evident in Fig. 3b than in Fig. 3d, constitutes a key point of the spectra of the window: the lower the amplitude of the oscillations, the lower the alteration of the windowed signal.

The so-called *rotate-translate* procedure constitutes an alternative strategy to minimize leakage in the case of finite sequences [10]. The procedure is illustrated in Fig. 4.

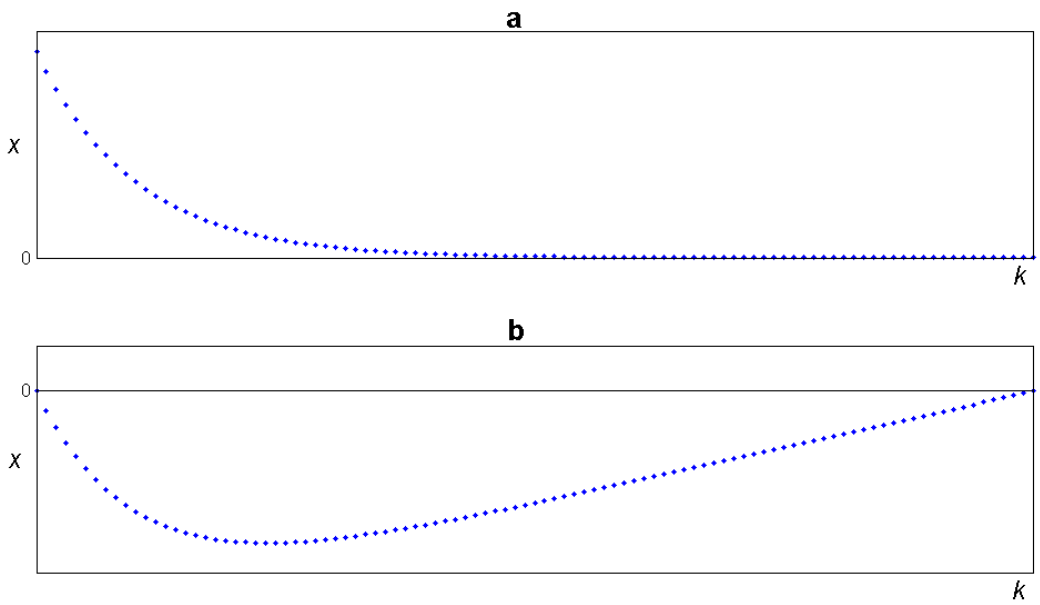

Fig. 4 Finite sequence with sharp discontinuity between the last and the first points (a); how the rotate-translate procedure may reduce this discontinuity (b) and the consequent spectral leakage.

Convolution

The analysis of the *convolution* operation is necessary to further evidence the potentialities of FT.

As it was mentioned in the Introduction section, it often happens that a measured signal results from a peculiar 'mixing', rather than superimposition, of individual signals relative to different sources. In many cases, convolution accounts for the way how two 'pure' signals combine with each other to give the resulting signal; furthermore, convolution of two sequences may be intentionally performed to reach a variety of goals. In mathematic terms, convolution is a multistep operation, consisting of:

- *folding*: reversing one of the two sequences to be convolved;
- *displacement*: shifting of the reversed sequence along the other one, by integer values that constitute the index of the resulting convolution sequence *y*;
- *multiplication*: point by point product of the values of the two sequences;
- *integration*: calculation of the overlap area as the sum of the point by point products: the result of the sum constitutes the value of the convolution sequence *y* at that index

Fig. 5 reports in graphical form these steps, through which convolution is realised.

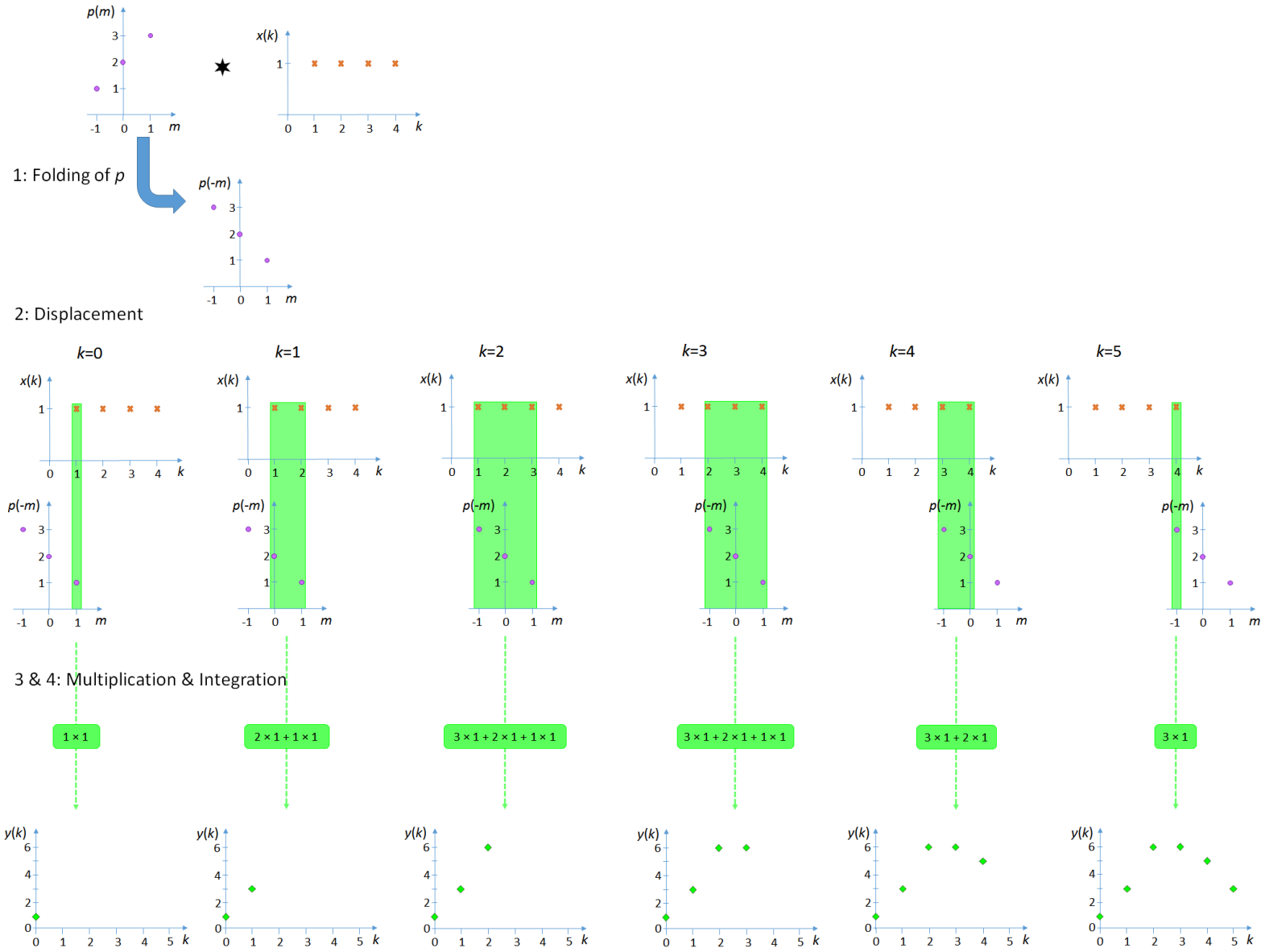

Fig. 5 Graphical representation of the steps involved in the convolution of two sequences p and x to give the sequence y.

The mathematic formulation of convolution of two sequences *x* and *p* is expressed by Eq. (3):

$$y(k) = x(k) \star p(k) = \sum_{m=-M}^{M} [p(m) \times x(k-m)] \qquad (3)$$

where the symbol ✶ stands for convolution operation, and where the number of points of the $p(k)$ (*p* for short from here onwards) sequence is $P = 2M+1$; the number of points of the *x* sequence is *Q*, and the number of points of the resulting *y* sequence is equal to $L = P+Q-1$ (actually, *y* may be prolonged by zeroes left and right the *L* points).

The convolution theorem

We cited above that it is much more advantageous to perform some mathematic operations in the alternative domain of the frequencies, than in the original domain of the signal. In the case of the convolution operation, we take advantage of the *convolution theorem*, sketched in Fig. 6, which can be summarized as follows: the spectrum expressing convolution between two sequences can be obtained through the multiplication of the relevant spectra, frequency by frequency [d].

In detail, given two sequences *x* and *p*, the convolution theorem requires the following steps[e]:

i) calculation on the relevant spectra: $X(h)=\mathrm{FT}[x(k)]$ and $H(h)=\mathrm{FT}[p(k)]$;

ii) multiplication of the two spectra term by term, i.e., frequency by frequency, to give the spectrum $Y(h) = X(h) \times H(h)$;

iii) inverse transform of the spectrum $Y(h)$: $y(k)= \mathrm{FT}^{-1}[Y(h)]$.

---

[d] Actually, this operation is most conveniently performed on the spectra represented in terms of complex numbers, rather than of sines and cosines. As in Part 1 of this series, in this paper we make use of sines and cosines to describe how FT works, but it must be recalled that this is equivalent to alternative representations, such as the one based on complex numbers. For the relationships existing among the different representations, the reader is referred to Ref. [3].

[e] Note again that, though we often refer only to magnitude spectra, both magnitude and phase spectra have to be used here (*X, H, Y*) and anywhere else, unless otherwise explicitly specified.

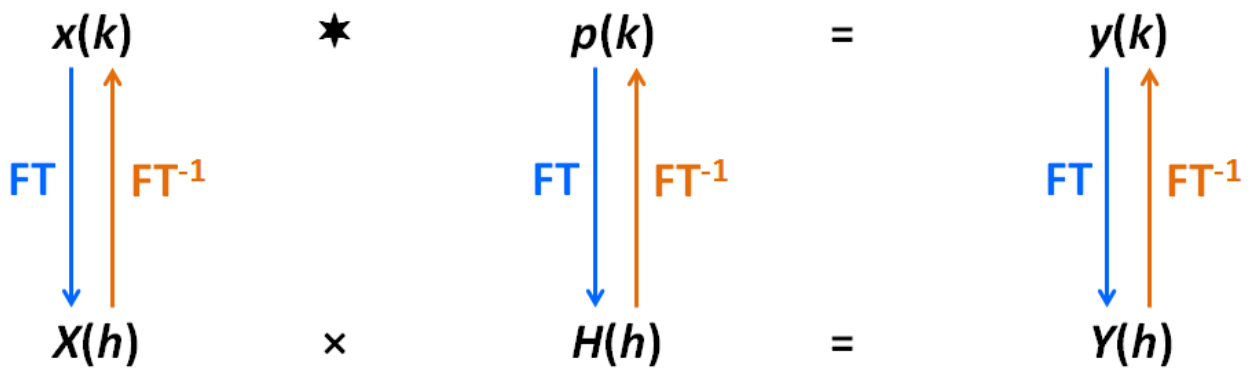

Fig. 6 Schematic representation of the convolution theorem.

A graphical example of the application of the convolution theorem, involving two sequences, *x* and *p,* is reported in Fig. 7.

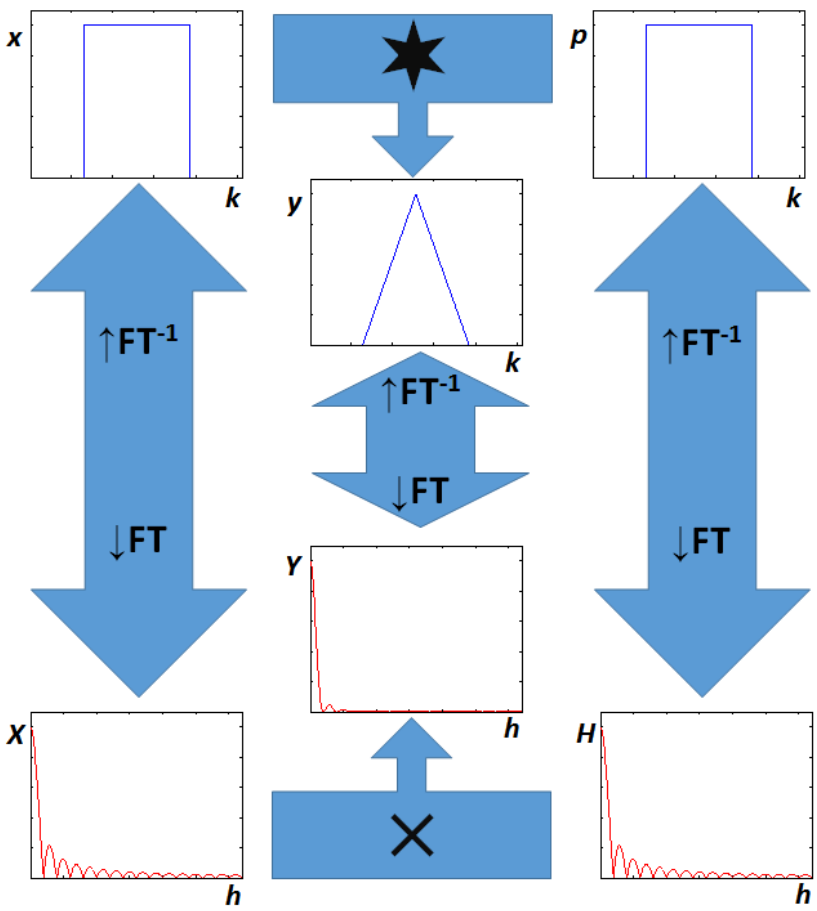

Fig. 7 Graphical example of the convolution theorem. For the sake of simplicity, in this graphical exemplification only the magnitude spectra are reported.

Fig. 7 highlights the equivalence between the convolution of x and p in the original domain (upper portion of the figure), in agreement with the definition given in Eq. (3), and the convolution performed by exploiting the convolution theorem (lower portion of the figure), i.e., by multiplying frequency by frequency the spectrum of x, $X(h)$, with the spectrum of p, $H(h)$.

According to the scheme in Fig. 6 and to the relevant discussion, Eq. (4) expresses the mathematic steps when applying the *convolution theorem*:

$$y(k) = L \times \mathrm{FT}^{-1}\{\mathrm{FT}[x(k)] \times \mathrm{FT}[p(k)]\}(k) = x(k) \ast p(k) = p(k) \ast x(k) \qquad (4)$$

where x and p are supposed to be equal to 0 outside Q and P points, respectively; y will be equal to 0 outside an interval consisting of $L = P+Q-1$ points.

Digital Filters

In Fig.7, the sequence x, once undergone to convolution with sequence p, typically a *filter*, leads to the sequence y. The spectrum of the filter, $H(h) = \mathrm{FT}[p]$, is called *transfer function*, which is nothing else than the *filter spectrum*: the multiplication of $\mathrm{FT}[x]$ by the transfer function leads to $\mathrm{FT}[y]$. The key question is: what does convolution between two sequences mean in physical terms? After illustrating how to perform convolution, we get now to the point.

Filtering is usually performed by exploiting the convolution theorem. The *digital filtering* issue [2,5,9] constitutes a topic of huge importance in the treatment of signals and data. The most widely used digital filters are *low-pass filters* or *band-pass filters*, which remove undesired frequencies from a signal. Low-pass filtering is a very profitable operation in the case of the presence of *random noise*. This may be identified with the *random errors* in many cases; random noise affects the signal introducing spurious high frequency components. Low-pass digital filters more flexibly substitute for the analog low-pass filters that are inserted in the circuits of analog instrumentation.

Digital low-pass filtering is a very common operation in experimental frames. The components of interest, suitable to represent a signal or sequence of data with a certain shape, are most often accounted for by lower frequencies than those ascribed to random noise. It should be noticed that random noise is always present in data of chemical interest; differently structured

noises are met with in different frames, which are differently named (white noise, pink noise, red or Brownian noise, blue noise, etc.) based on the shape of the noise spectrum [11]

Fig. 8 sketches a low-pass filtering operation, performed using a rectangular transfer function (this shape is often referred to as *boxcar*), with the consequent effect on a measured sequence affected by high frequency noise.

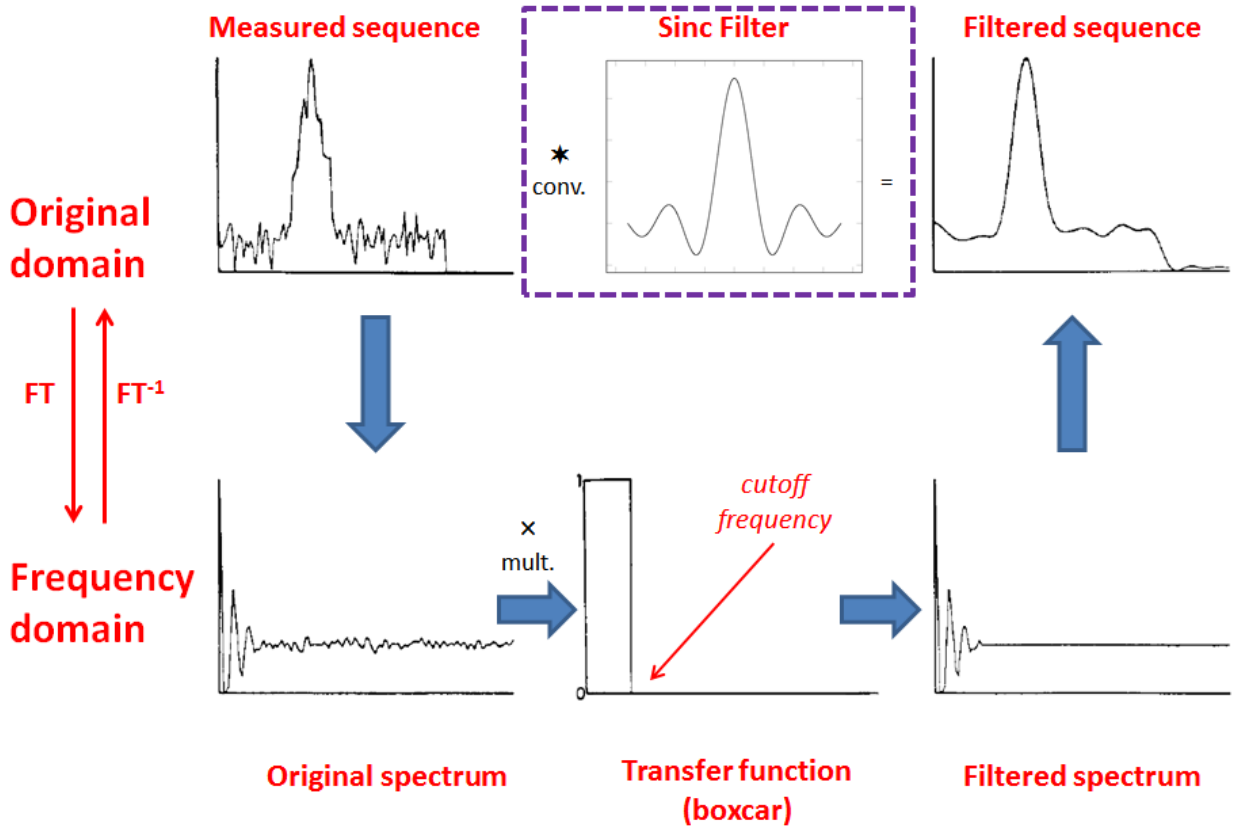

Fig. 8 The original noisy signal is either directly convolved with a sinc function or, in equivalent way, through the convolution theorem, by means of a rough boxcar: the spectrum of the signal is multiplied by that of the sinc function (adapted from Ref [12]).

Coherently with the convolution theorem (Fig. 6), the path followed to perform the low-pass filtering operation is highlighted by the blue arrows in Fig. 8: the measured sequence in the original domain is transformed into the corresponding spectrum in the frequency domain. In turn, this latter one is multiplied, point by point, by the boxcar transfer function. From the resulting filtered spectrum, it is clear that the boxcar transfer function does not alter the frequency components of the spectrum till a value below which the information content necessary to reconstruct the 'clean' sequence is supposedly brought, and sets the coefficients of the higher frequencies to 0.

This is actually a very coarse filtering method that, however, is quite often used, even leading to satisfactory results when the components of the noise to filter off are well separated from the useful ones. In these cases, the *cutoff frequency*, i.e., the frequency value above which the magnitude values are set to 0, is located in a region of the spectrum where the magnitude values are equal or very close to 0, and lower frequencies constitute the whole 'useful' portion of the signal.

In the dashed frame in the same Fig. 8 the inverse Fourier transform of the boxcar transfer function, namely the *sinc filter*[f] is included: an alternative path can be followed to obtain the same result, i.e., to obtain the same filtered sequence, which consists of convolving the measured sequence with a sinc filter. It gives reason of the fact that if the cutoff frequency of the boxcar transfer function is located where the magnitude values are different from zero, artefacts in the filtered sequence are introduced: the higher the magnitude values in proximity to the cutoff, the higher the intensities of the side lobes in the sinc filter. In this case, the frequencies are truncated too abruptly, and the side lobes present in the sinc filter induce oscillations in the filtered sequence, due to Gibbs phenomenon.

Some examples of other simple transfer functions used to perform low-pass filtering are shown in Fig. 9, together with the resulting filtered sequences. The transfer functions in Fig. 9 are among the simplest ones in the big number of transfer functions that can be used for this purpose.

[f] The sinc function is commonly defined for $x \neq 0$ by $\mathrm{sinc}(x) = \sin(x)/x$, while the value at $x = 0$ is defined as the limiting value $\mathrm{sinc}(0) = 1$. The Fourier Transform of the sinc function is the rectangle function, i.e. the boxcar.

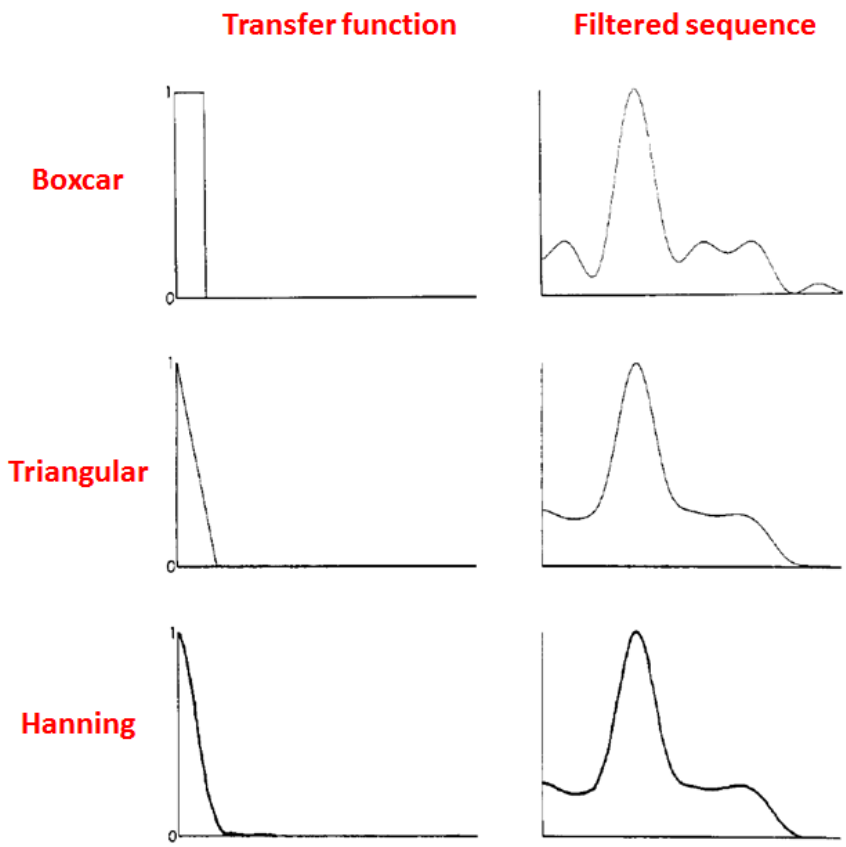

Fig. 9 Results obtained by low-pass filtering the measured sequence of Fig. 8 with different transfer functions (adapted from Ref [12]).

In conclusion, the design of the most suitable low-pass filters or of the corresponding transfer functions aims at introducing as low as possible artefacts in the signal bearing useful information, as it would be recorded whether the noise were not present.

As mentioned above, in addition to those performing low-pass filtering, filters have been designed to differently manipulate the input *x* sequence: differentiating filters, integrating filters, etc. have been designed and optimised for different possible cases. As an example, Fig. 10 sketches the transfer function of a differentiating filter (Fig 10b), together with the result (Fig 10c) obtained by its application to a couple of peaks (Fig 10a).

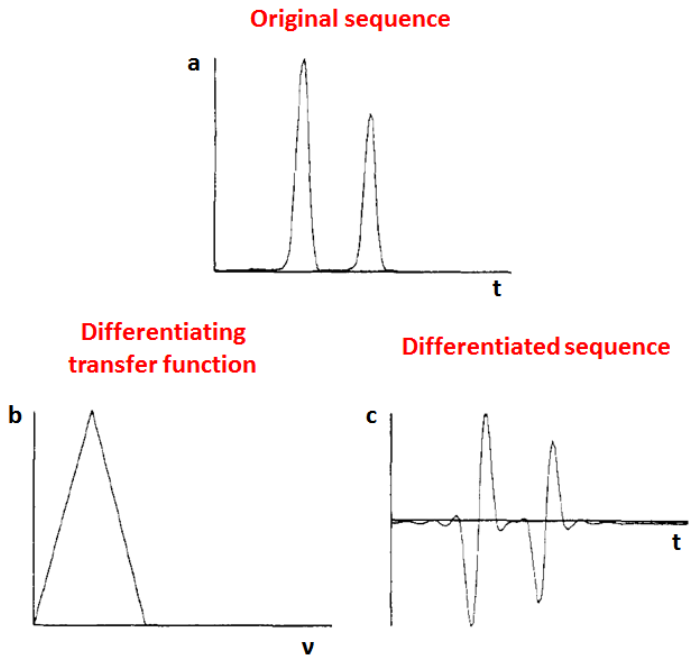

Fig. 10 Example of the application to a couple of peaks (a) of the transfer function of a differentiating filter (b), together with the resulting differentiated sequence (c) (adapted from Ref. [12]).

We are aware of the possibility that confusion arises from what written so far about windowing and filtering, since the description of both operations has induced to often shift from the original domain to the frequency domain and vice versa. In the attempt to make the matter as clear as possible, Scheme 1 gives an idea of the computational analogies and of the deep, not only conceptual, differences between the two operations, at the same time. Actually, both windowing and filtering make use of the convolution theorem; however, they are completely different operations, using similar tools in 'reverse order' we could say, and which are used to completely different purposes.

		WINDOWING		
SEQUENCE	×	WINDOW	→	WINDOWED SEQUENCE
↓↑		↓↑		↓↑
SEQUENCE SPECTRUM	✶	WINDOW SPECTRUM	→	WINDOWED SEQUENCE SPECTRUM
		FILTERING		
SEQUENCE	✶	FILTER	→	FILTERED SEQUENCE
↓↑		↓↑		↓↑
SEQUENCE SPECTRUM	×	TRANSFER FUNCTION (FILTER SPECTRUM)	→	FILTERED SEQUENCE SPECTRUM

↓ stands for FT

↑ stands for FT^{-1}

× stands for point by point multiplication

✶ stands for convolution operation

Scheme 1. What happens in windowing and in filtering operations.

Maybe it is not redundant to schematically summarise the issue, even running the risk of repeating some concepts. Let's recall that windowing is used to truncate a sequence before calculating the relevant spectrum, and that the windowed sequence is given by the point by point multiplication between the sequence *x* and the window *p*. Due to the reversible character of the FT operation, the reverse of what shown in Fig. 6 also holds: the convolution between the spectra of *x* and of *p* corresponds to the spectrum of the sequence obtained by multiplying point by point *x* and *p*. Therefore, the convolution theorem can be applied to windowing: the spectrum of the windowed sequence can be also obtained by convolving the sequence spectrum with the window spectrum. For this reason, knowing the shape of both the window and the window spectrum allows one to understand what happens both in the original and in the frequency domains. Making reference to Fig. 2 and Fig. 3, this accounts for the effect of the oscillations in Fig. 3b (spectrum of the rectangular window) on the corresponding spectrum of Fig. 2d. The side lobes of the window spectrum cause the arising of spurious frequencies in the spectrum of the windowed sequence, which in turn are responsible for the Gibbs phenomenon, i.e., for the spurious oscillations in the reconstructed sequence.

Smoothing filters

Quite a common way to apply low-pass filtering consists in convolving the signal with a short length filter that 'moves' along the signal itself, piece by piece, one point at a time, filtering off the high frequencies: *Moving Average* (*Smoothing*) *Filters*. A sequence consisting of a given number of points of the signal is convolved with an equally long sequence constituting the filter. Such an operation is nothing else that the already discussed convolution between the sequences expressing subsequent pieces of the signal and the *p* sequence of the filter. However, the widespread use of similar operation and of the relevant denomination deserves a specific treatment.

In this frame, a number of filters are widely diffused. Limiting once more the exam to low-pass filters, also when following this 'piecewise' approach the most common filter is the very simple rectangular one. The way how the smoothing average low-pass filter operates is illustrated in Fig. 11. The moving filter constitutes itself the convolution sequence *p*. In practice, using a rectangular 5 point long *p* sequence, every *y* filtered point is obtained by re-calculation as the mean value of 5 points: a convolution of five points of the original sequence *x* with the filtering sequence *p* is performed. Assuming 0 index for the point of *p* coincident with the point of *x* to recalculate, *p* values are set to 1 for index assuming integer values from -2 to +2 and to 0 outside this interval. As noticed above, Eq. (3) expresses that points of the sequence *x* are convolved with the 5 point long *p* sequence constituting the filter, to give the *y* filtered sequence. Noteworthy, the number of points of *p* in the moving average operation is always odd, in a way that, for each *k* value, $y(k)$ is the average value calculated including the same number of points both on the left and on the right of $x(k)$.

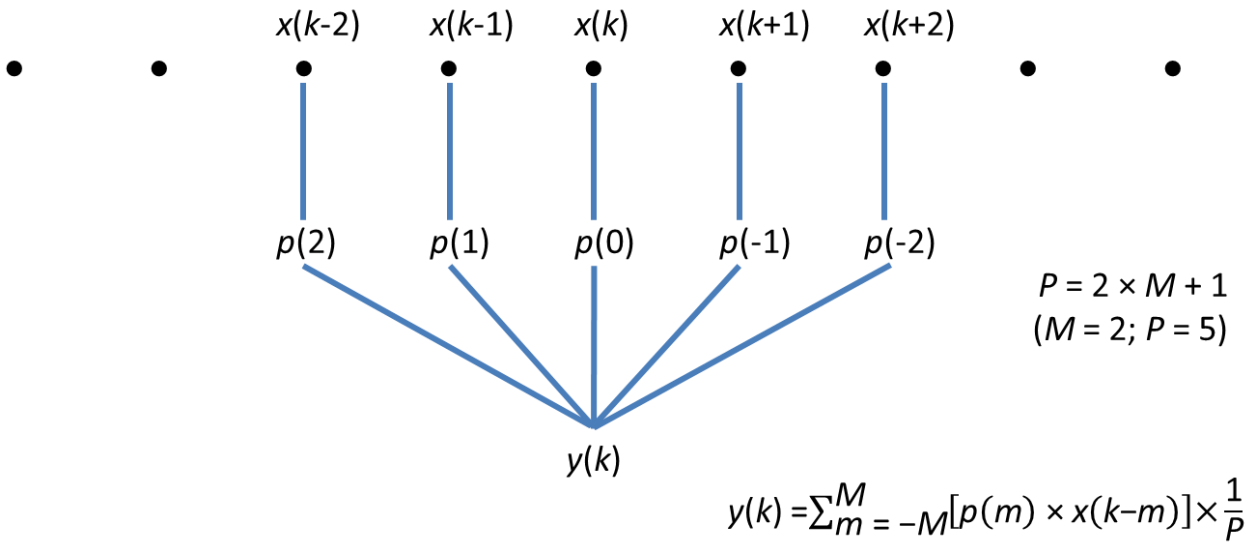

Fig. 11 Scheme of the moving average filter.

Since a convolution operation is performed, also in this case the convolution theorem can be applied. The transfer functions that result for different numbers of points constituting the rectangular convolution filter are reported in Fig. 12.

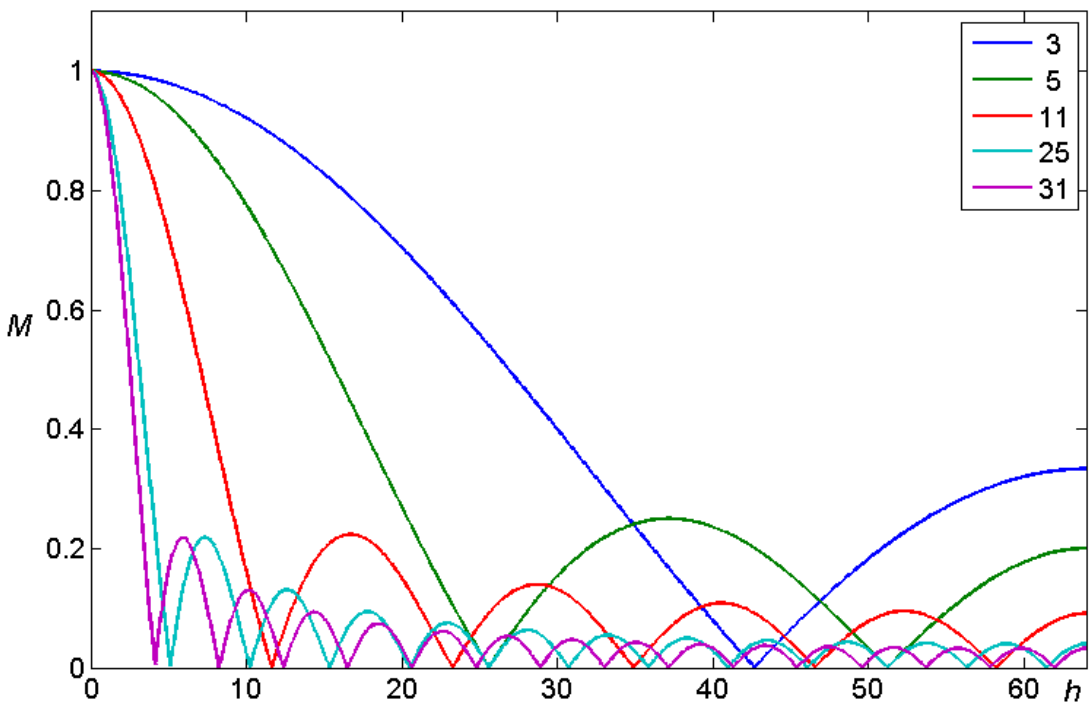

Fig. 12 Magnitude spectra of transfer functions corresponding to the 3, 5, 11, 25, and 31 point-long rectangular convolution smoothing filters.

Looking at the plots in Fig. 12, the analysis of what the more or less explicit convolution operation actually implies, does not seem redundant with respect to the simple "mean of 3, 5, 11, 25 or 31 subsequent points" operation. Since similar transfer functions are the spectra of rectangular filters, it is not surprising that they have the same shape as the window spectrum reported in Fig. 3b. Making reference to Scheme 1, however, in the windowing operation the spectrum of the window is convolved with the spectrum of the sequence, while in this case the spectrum of the window (transfer function) is multiplied by the spectrum of the sequence, exactly as it happens in filtering. In fact, moving average smoothing corresponds to low-pass filtering, as described in the lower part of Scheme 1.

The plots in Fig.12 all represent transfer functions relative to low-pass filters, i.e., filters that smooth the signal, aimed at cutting off the highest frequencies. The smoothing operation involving an increasing number of points may 'filter too much', only considering lower and lower frequencies. In the limit, a *p* sequence that is as long as the signal only gives the mean value of the signal itself. On the opposite, a *p* sequence consisting of 1 point… does not filter anything, only 'copying' the *x* sequence into the *y* one.

In addition to moving average, many other smoothing filters have been proposed in the literature; they constitute a more sophisticated and often effective portion of the issue, and a detailed description of them is out of the aims of the present contribution. In an article published in 1964 in the journal *Analytical Chemistry*, a number of different, still widely used and quite effective filtering sequences were proposed by Abraham Savitzky and Marcel J. E. Golay, which are known as Savitsky-Golay filters [13]. This article is still one of the most widely cited contributions in the field of Analytical Chemistry [14].

A Gaussian curve also represents a possible convolution filter alternative to the rectangular one, suitable for smoothing purposes: Gaussian smoothing may be modulated through the standard deviation of the Gaussian curve [15]. Compared to the rectangular moving average filter, a Gaussian filter provides for gentler smoothing: the relevant spectrum gives reason of one of the most attractive features. Fig. 13 compares the transfer functions, in terms of magnitude, for a rectangular filter with width 5 and for a Gaussian filter with standard deviation of 3. Both filters attenuate the high frequencies more than the low ones, but the Gaussian filter transfer function shows no oscillations (absent or poor leakage): the Gaussian filter and the corresponding transfer function are a Gaussian and (half a) Gaussian, respectively. This implies that side lobes are absent

in the filter spectrum, which minimises the spurious oscillations arising in the filtered signal (limited evidence of Gibbs phenomenon) [15].

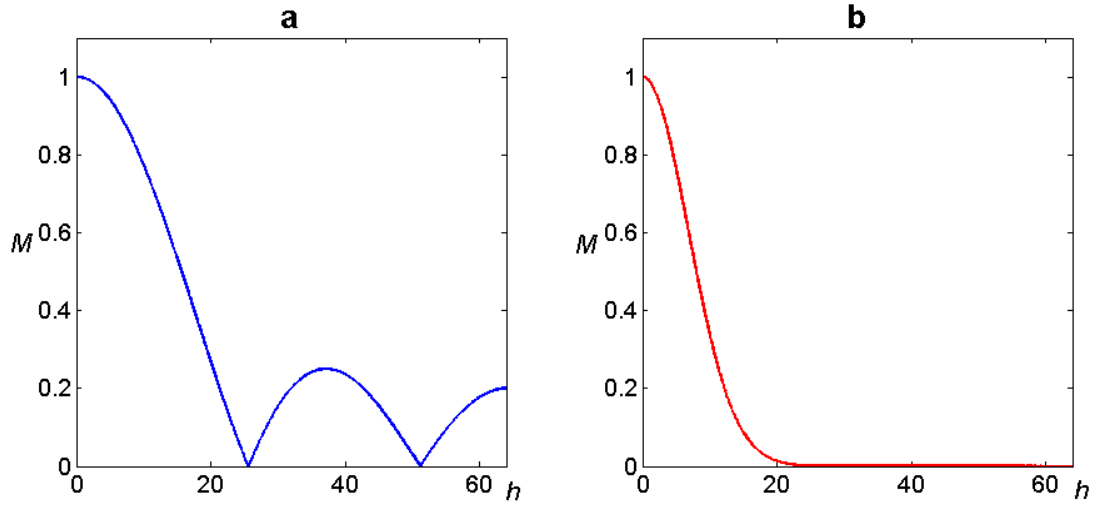

Fig. 13 Magnitude spectra of a rectangular filter with width 5 (a) and of a Gaussian filter with standard deviation of 3 (b).

Spontaneous convolutions

In addition to many cases of data treatment in which a convolution of two sequences is intentionally performed to whatever scope, convolution often occurs 'spontaneously'. On the one hand, some signals arise by simple sum of two or more components and, on the other hand, other signals are the result of convolution. In other words, it may happen that the signal recorded actually results from a 'blend' of two or even more components. Each one of them accounts for one 'phenomenon' which, by convolution with each other, generates the measured signal.

A typical example may be observed in UV-Vis spectroscopy, due to the effect of the finite width of the exit slit of a monochromator on the spectrum of a substance. Fig. 14a sketches what happens: the polychromatic light, by traversing the diffraction grid, is 'decomposed' in such a way that radiations at different wavelengths are addressed to different directions, according to different deflection angles.

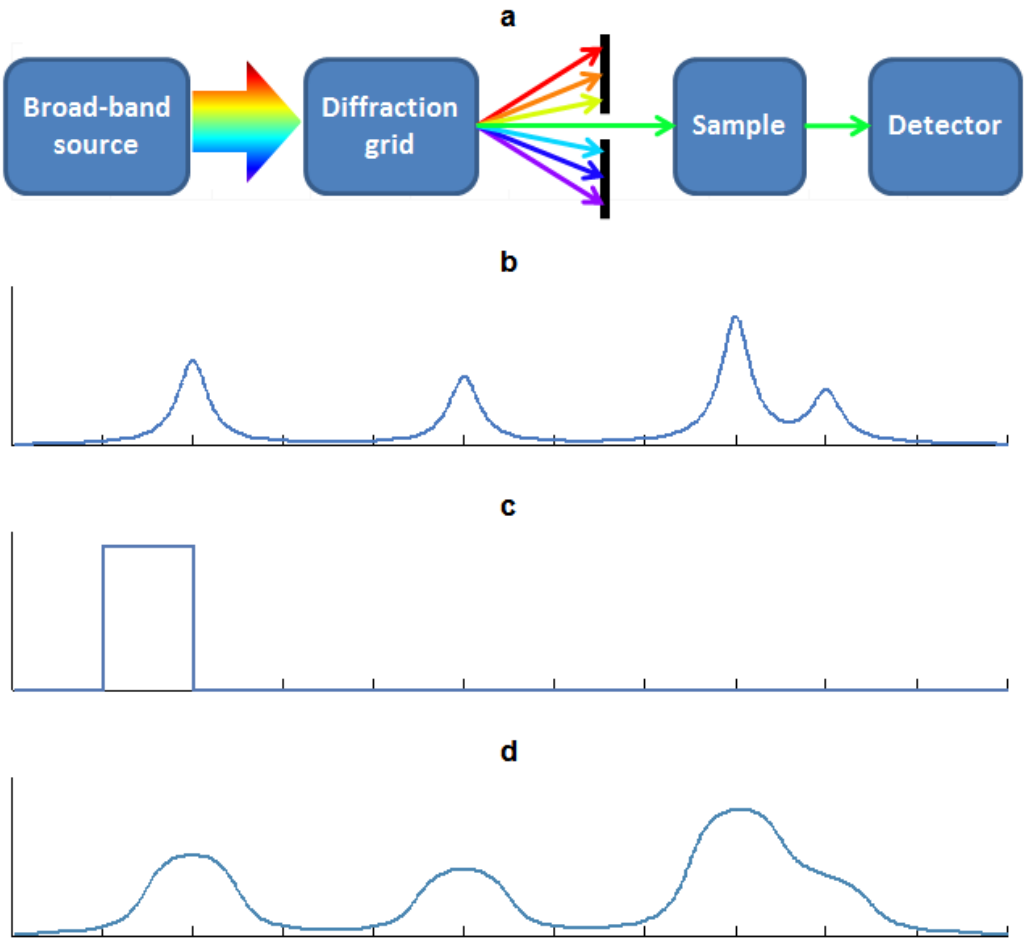

Fig. 14 Decomposition of polychromatic light by a diffraction grid and selection of a narrow wavelength range by the monochromator slit (a); in (b) a simulated 'ideal' spectrum is depicted; by convolution with the sequence accounting for the monochromator slit in (c) the actual spectrum in (d) is recorded.

The selection of the radiations entering the sample occurs through a slit: only the radiations along the directions that cross the slit reach the sample. For a given dispersion, the narrower the slit, the narrower the selected range of wavelengths. With such a system, true monochromatic radiation would be only obtained by an infinitesimal slit width, which would however lower to zero the intensity of the radiation. The compromise implies that a finite interval of wavelengths should be accepted to pass across the slit and to reach the sample. As a result, broadening of the absorption bands is observed. Fig. 14b reports the theoretic spectrum, recorded by an ideal selection of one single radiation wavelength at a time, and Fig. 14c reports the square function accounting for the slit. The broadened recorded spectrum, reported in Fig 14d, results from the convolution of the theoretic spectrum with the square function accounting for the slit.

Similarly to the finite width of a slit in a spectrometer, the width of the tip of the probe affects the resolution in an Atomic Force Microscopy (AFM) image. In fact, the shape of the tip is convolved with the true surface profile, leading to record a 'smoothed' image, as it is sketched in Fig. 15.

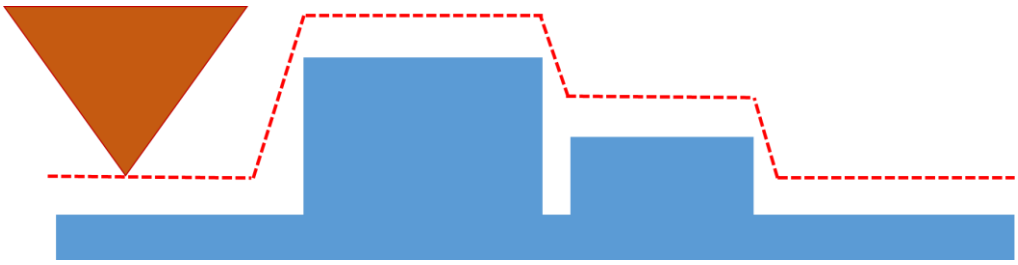

Fig. 15 Schematic representation of the convolution of the tip shape with the surface profile in AFM.

A further example of an analytical signal that can be expressed as the convolution of two functions is given by a chromatographic peak. Its shape, around which a huge literature amount has been written, may be expressed by convolution of the injection profile of the species with the impulse response of the chromatographic system; this represents the peak shape under the condition that a Dirac delta or impulse function, δ, [1, 2] represents the injection profile.

In addition to the examples reported above, many other cases may be cited, in the fields of electrochemistry, NMR and X-ray spectroscopies, crystallography, seismology, image processing, and remote sensing.

Deconvolution

In the cases like those of the previous examples, it may be useful or even necessary to separate the individual contributions to the overall measured signal, in order to achieve UV-Vis spectra, AFM images or chromatographic peaks that are not 'polluted' by undesired effects. This allows the achievement of more correct information about the observed sample and about the physical laws determining the responses. Since, as above illustrated, 'mixing' comes out from a convolution operation, it may be fruitful to operate *deconvolution*, which is the process used to reverse the effects of convolution.

Re-examining the example of the UV-Vis spectrum reported in the previous section, the ideal spectrum in Fig. 14b may be obtained by deconvolving the slit sequence in Fig. 14c from the recorded spectrum in Fig. 14d. The convolution operation does not present particular

computational difficulties, except for eventual computational load, even when performed in the original domain [see Eq.(3)]. Conversely, deconvolution requires the solution of a system of linear equations that becomes increasingly heavy at increasing the number of points constituting the sequences. On the other hand, in view of the convolution theorem reported in Eq (4), the following equations hold:

$$p(k) = L \times \mathrm{FT}^{-1}\{\mathrm{FT}[y(k)] / \mathrm{FT}[x(k)]\}(k) = y(k) \bigstar^{-1} x(k) \qquad (5)$$

and

$$x(k) = L \times \mathrm{FT}^{-1}\{\mathrm{FT}[y(k)] / \mathrm{FT}[p(k)]\}(k) = y(k) \bigstar^{-1} p(k) \qquad (6)$$

where $\bigstar^{-1}$ is the symbol used to indicate the deconvolution operation.

A sophisticated example of the potentialities of convolution and deconvolution operation is found in an 'exercise' of Donald Smith [16]. In Fig. 16 two impulses located at the relevant $E_{1/2,r} \approx E°$, with intensity proportional to the concentration of the corresponding electroactive species (Fig. 16c), are convolved with the so-called 'Nernstian broadening', i.e., $1/\cosh^2(j/2)$, j representing the distance of the polarising potential from $E_{1/2,r.}$ (Fig. 16b) .[g] In turn, additional convolution with $t^{-1/2}$ (indicated, not shown), accounting for linear semiinfinite diffusion, leads to the well-known linear sweep voltammetric response (Fig. 16a) [17]. The two impulses may be the starting point or, conversely, they may be the final goal, resulting from subsequent deconvolution of $t^{-1/2}$ and of the plot in Fig. 16b from the (recorded or constructed) signal (Fig. 16a).

[g] $E_{1/2,r}$, the so-called half wave potential, is a good experimental approximation of the standard potential in the case of a reversible charge transfer, differing from $E°$ as far as the activity coefficient and the diffusion coefficients of the species of the redox couple involved are different from one another; $\cosh x = (e^x + e^{-x})/2$.

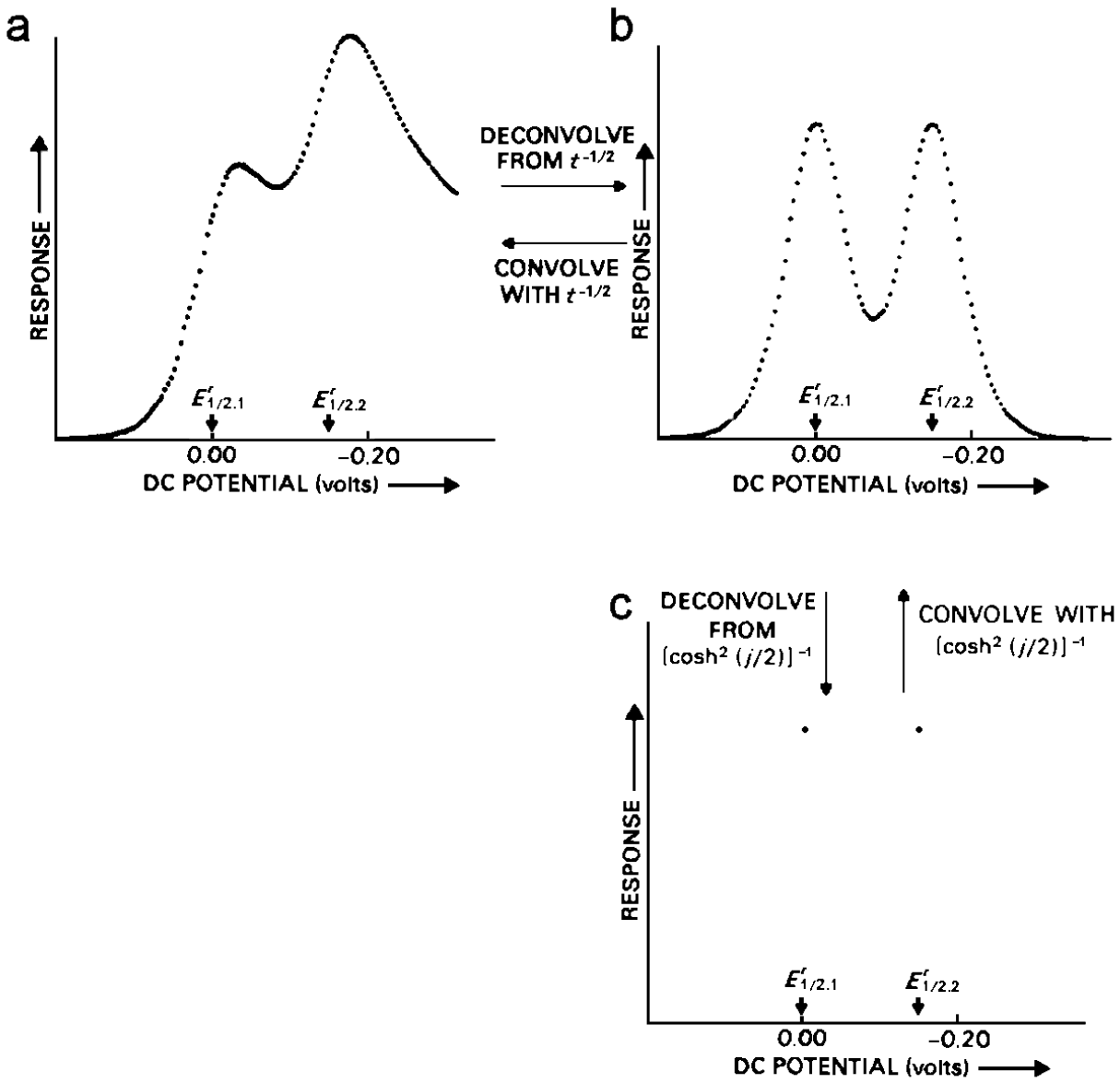

Fig. 16 From impulses to 'Nernstian broadened' sequences and to linear sweep voltammetric response, by subsequent convolution operations. The opposite path is followed by the relevant deconvolutions (adapted from Ref. [16]).

The result of deconvolution is fascinating, making an overall response coincide with impulses located at $E_{1/2,r}'$, experimental approximation of E°' of the two redox couples involved (Fig. 16c). The self-deconvolution operation, leading to impulses, is a potentially dangerous one, involving computational criticisms arising, for instance, by calculation of ratios between very small numbers[h], by strong effect of noise or of rounding.

[h] For example, $8 \times 10^{-15} / 2 \times 10^{-18}$, where both values are not significant, leads to 4×10^{3}, which is a high value that could strongly affect the final result.

Refs. [18,19] report further possible manipulations of simulated and experimental, reversible or non reversible voltammetric responses, by convolution and deconvolution procedures.

Further FT- based manipulations of signals

It very often happens that signals obtained by whatever analytical technique, like spectroscopy, electrochemistry, chromatography or others, consist of peaks or bands that are severely overlapped to each other. Once the shape of the single peak or band is known, deconvolution by the function accounting for the proper shape could lead, in principle, to single impulses, similarly to the electrochemical case illustrated above. Fig. 17 shows an example in which a deconvolution algorithm based on FT is suitable to obtain very satisfactory resolution of overlapped peaks, as long as two impulses or very narrow peaks are obtained [20].

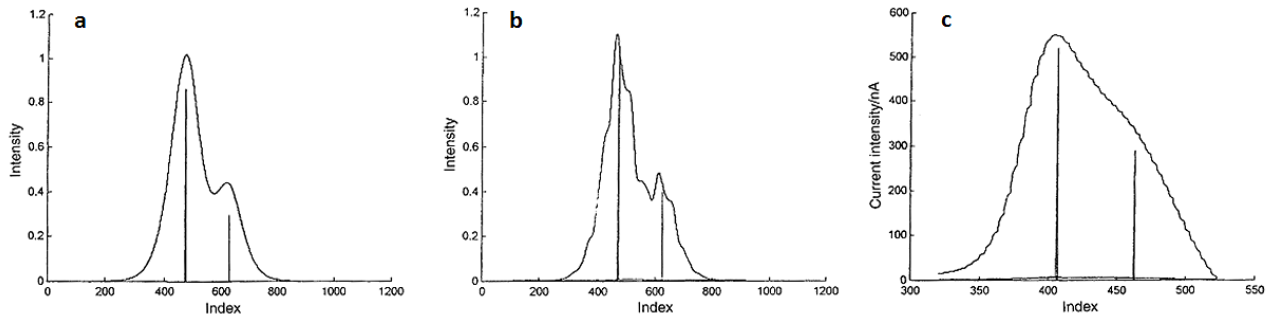

Fig. 17 (a) simulated partially overlapped differential pulse polarographic signals; (b) noise is superimposed to (a); (c) experimental differential pulse polarographic response for a mixture of cadmium(II) and lead (II). The results of suitable deconvolutions are superimposed: impulses are obtained for (a) and (b), very narrow peaks for (c) (adapted from Ref. [20]).

Another quite appealing operation is made possible by applying subsequent FT and FT^{-1} operations: the *trigonometric interpolation* [21]. Due to the property of FT to bear a number of sine and cosine components equal to the number of points of the analysed sequence, a signal consisting of *N* points exhibits a spectrum consisting of the same number of points. Going back to the original domain by FT^{-1}, a sequence with *N* points is reconstructed. However, the addition to the spectrum of a number of 'fictitious' frequency components with amplitude equal to 0 does not

alter it, since it does not modify the frequency content of the original signal. On the other hand, by inverse transform a signal consisting of a higher number of points is reconstructed. The extreme values of the interval of the original signal are not altered, nor the shape is changed, since no operation on the frequencies that describe the actual signal has been performed. The points in the reconstructed signal are closer to each other, allowing to more precisely identify the significant points of the signal itself, such as the location on the abscissa of relative maxima. Such an interpolation operation is also called *zero-filling* and is illustrated in Fig. 18.

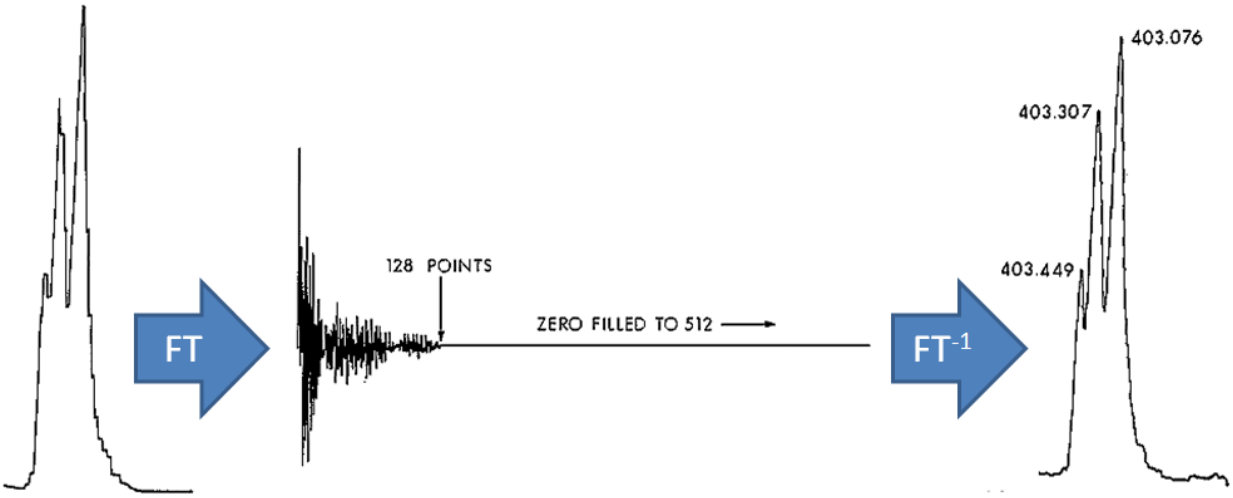

Fig. 18 A photodiode array only records 128 points around the Mn triplet located at 403 nm. The resolution of 100 μm of the rough detector system is unsatisfactory; trigonometric interpolation is of notable help (adapted from Ref. 21).

Additional complete, orthogonal sets of functions or sequences: further transforms methods

In manipulating a set of data or signals, different aims may be sought, such as calculating the spectrum of a signal, filtering the signal, compacting big amount of data, etc. FT is the most known and widespread transform technique in the frame of the analysis of signals, using sines and cosines as the orthogonal basis set, or equivalent representations through magnitude and phase vectors, or through complex numbers. However, this does not always constitute the best choice to the purpose: the use of other transform algorithms can be more suitable.

It has been already evidenced [1] that the transform techniques make use of a set of basis functions that are suitable to represent the original signal by a proper linear combination: making

best choice of the basis set is crucial. In this frame, it is well known that the intrinsically smooth cosine and sine functions are poorly suitable to account for sharp changes or discontinuities: the representation of a square wave is a typical example. Fig. 19 reports what is obtained by a higher and higher number of sine terms, which forces the Gibbs phenomenon to be less and less evident, becoming however effective only when quite a high number of terms is employed.

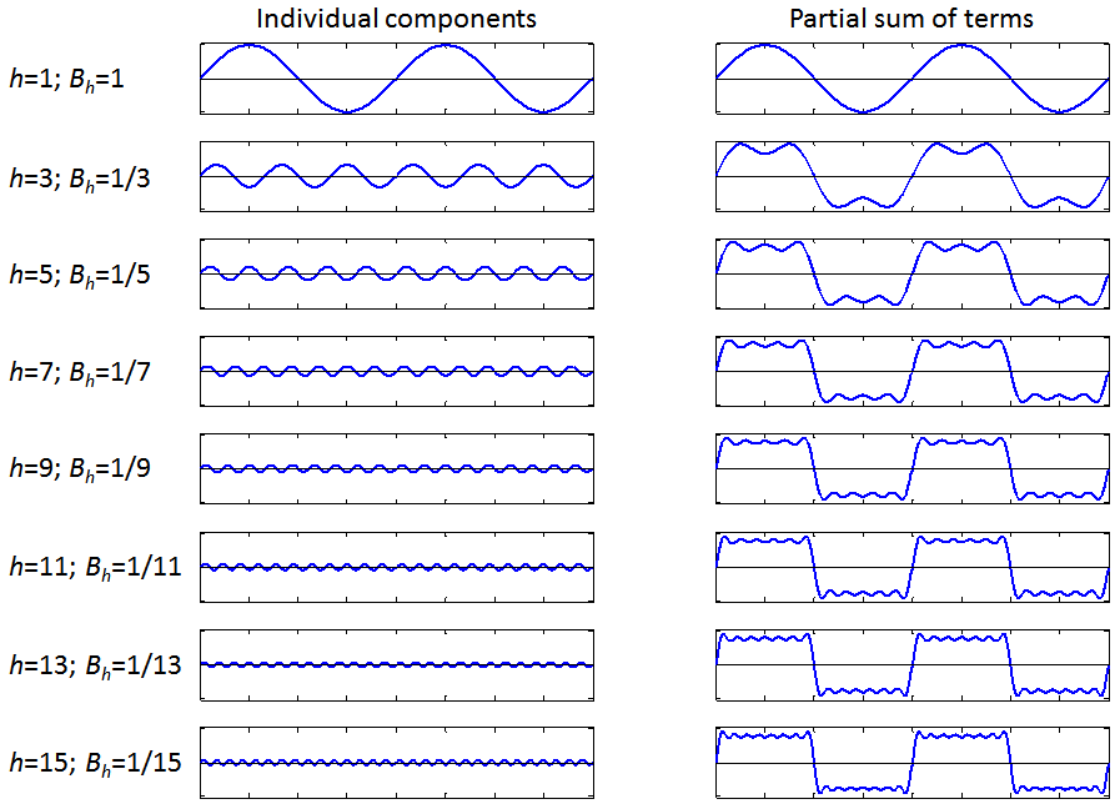

Fig. 19 Left column: the individual components in the Fourier series, right column: the partial sum of terms in the Fourier series.

It is evident that the more similar the shape of the set of basis functions to that of the signal, the lesser the number of terms necessary to achieve best fit of the signal itself. The reader is necessarily addressed to dedicated literature to find meaning and properties of additional basis sets, suitable to represent signals with peculiar trends through the relevant transform techniques [6,22,23]. Among these, which are called according to names of mathematicians developing the algorithms, let's cite *Rademacher*, *Walsh*, *Hadamard*, *Hilbert*, *Haar transforms*. In particular, the *Haar basis set* constitutes the first, simplest *wavelet*, from which *Wavelet Transform* method opened an unprecedented wide field of powerful signal processing techniques [23].

References

1. Seeber R, Ulrici A (2016) Analog and digital worlds: Part 1. Signal sampling and Fourier Transform. ChemTexts (2016) 2:18
2. Poularikas AD, Seely S (1994) Signals and systems. 2nd Ed. PWS-KENT, Boston
3. Weaver HJ (1983) Applications of discrete and continuous Fourier analysis. Wiley, New York
4. Brigham EO (1974) The fast Fourier transform. Prentice-Hall, Englewood Cliffs
5. Oppenheim Av, Schafer RW (1975) Digital signal processing. Prentice-Hall, Englewood Cliffs
6. Marshall AG (ed) (1982) Fourier, Hadamard, and Hilbert transform in chemistry. Plenum Press, New York
7. Griffiths PR, de Haseth JA (2007) Transform techniques in chemistry, 2nd Ed. Wiley, New York
8. Bracewell RN (1978) The Fourier transform and its applications, 2nd Ed. McGraw-Hill, New York
9. Hamming RW (1989) Digital filters, 3rd Ed. Dover Publ, Mineola
10. Hayes JW, Glover DE, Smith, DE, Overton MW (1973) Some observations on digital smoothing of electroanalytical data based on the Fourier transformation. Anal Chem 45:277-284
11. O'Haver TC A Pragmatic Introduction to Signal Processing, . https://terpconnect.umd.edu/~toh/spectrum/TOC.html
12. Horlick G (1972) Digital data handling of spectra utilizing Fourier transformations. Anal Chem 44:943-947
13. Savitzky A, Golay MJE (1964) Smoothing and differentiation of data by simplified least squares procedures. Anal.Chem 36:1627-1639
14. Larive CK, Sweedler JV (2013) Celebrating the 75th Anniversary of the ACS Division of Analytical Chemistry: A Special Collection of the Most Highly Cited Analytical Chemistry Papers Published between 1938 and 2012. Anal Chem 85:4201–4202
15. Fisher R, Perkins S, Walker A, Wolfar E, http://homepages.inf.ed.ac.uk/rbf/HIPR2/gsmooth.htm
16. Smith DE (1976) The enhancement of electroanalytical data by on-line fast Fourier transform. Anal Chem 48:517A-526A

17. Bontempelli G, Magno F, Mazzocchin GA, Seeber R (1989) Linear sweep and cyclic voltammetry. Ann Chim (Rome) 79:103-216
18. Pilo MI, Sanna G, Seeber R (1992) Analysis of cyclic voltammetric responses by Fourier transform-based deconvolution and convolution procedures. J Electroanal Chem 323:103-115.
19. Bentley CL, Bond AM, Hollenkamp AF, Mahon PJ, Zhang J (2014) Application of convolution voltammetry in electroanalytical chemistry. Anal Chem 86:2073-2081
20. Allegri D, Mori G, Seeber R (1996) Resolution of Partially Overlapped Signals by Fourier Analysis. Application to Differentialpulse Polarographic Responses. The Analyst 121:1359-1365
21. Horlick G, Yuen WK (1976) Fourier domain interpolation of sampled spectral signals. Anal Chem 48: 1643-1644
22. Seeber R, Ulrici, A (1999) Transform methods in the synthesis and elaboration of signals. Quim Anal 18:11-27
23. Walczak B. (Ed.) (2000) Wavelets in Chemistry. Elsevier, Amsterdam

 Click here to download Table Scheme_1.tif

WINDOWING				
SEQUENCE	×	WINDOW	→	WINDOWED SEQUENCE
↓↑		↓↑		↓↑
SEQUENCE SPECTRUM	✶	WINDOW SPECTRUM	→	WINDOWED SEQUENCE SPECTRUM
FILTERING				
SEQUENCE	✶	FILTER	→	FILTERED SEQUENCE
↓↑		↓↑		↓↑
SEQUENCE SPECTRUM	×	TRANSFER FUNCTION (FILTER SPECTRUM)	→	FILTERED SEQUENCE SPECTRUM

↓ stands for FT

↑ stands for FT^{-1}

× stands for point by point multiplication

✶ stands for convolution operation

Figure

Click here to download Figure Figure_1.tif

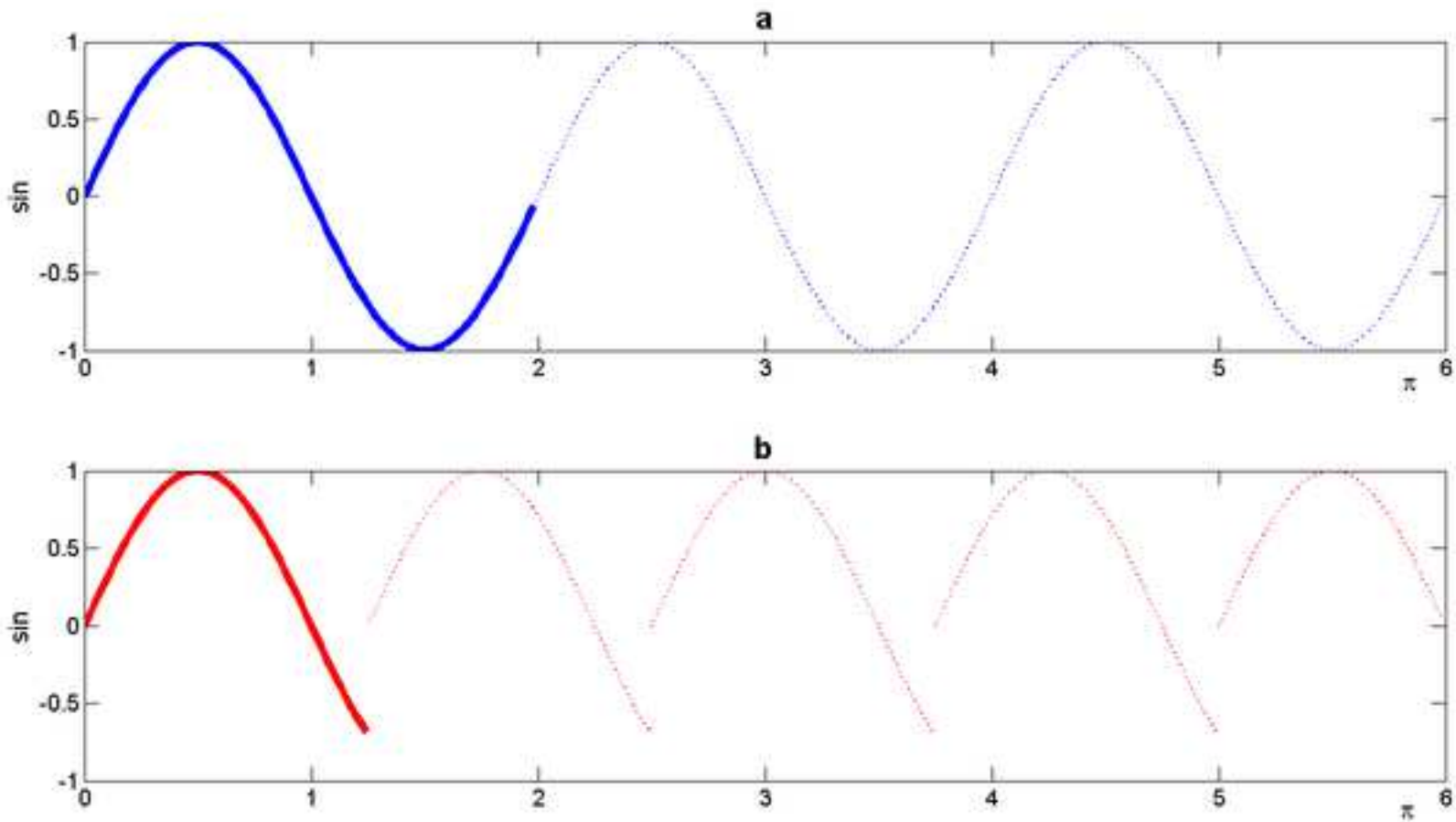

Figure

Click here to download Figure Figure_2.tif

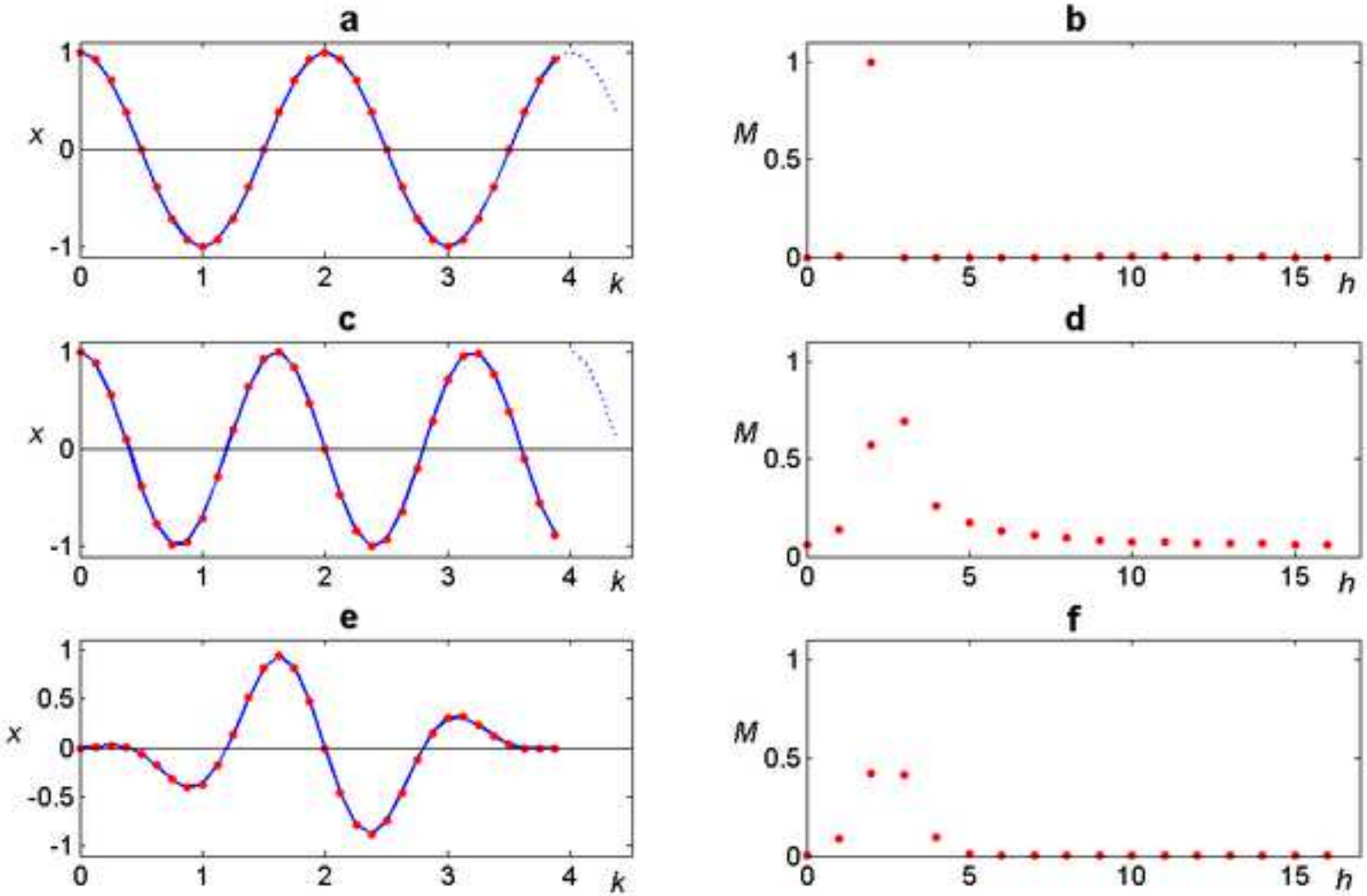

Figure

Click here to download Figure Figure_3.tif

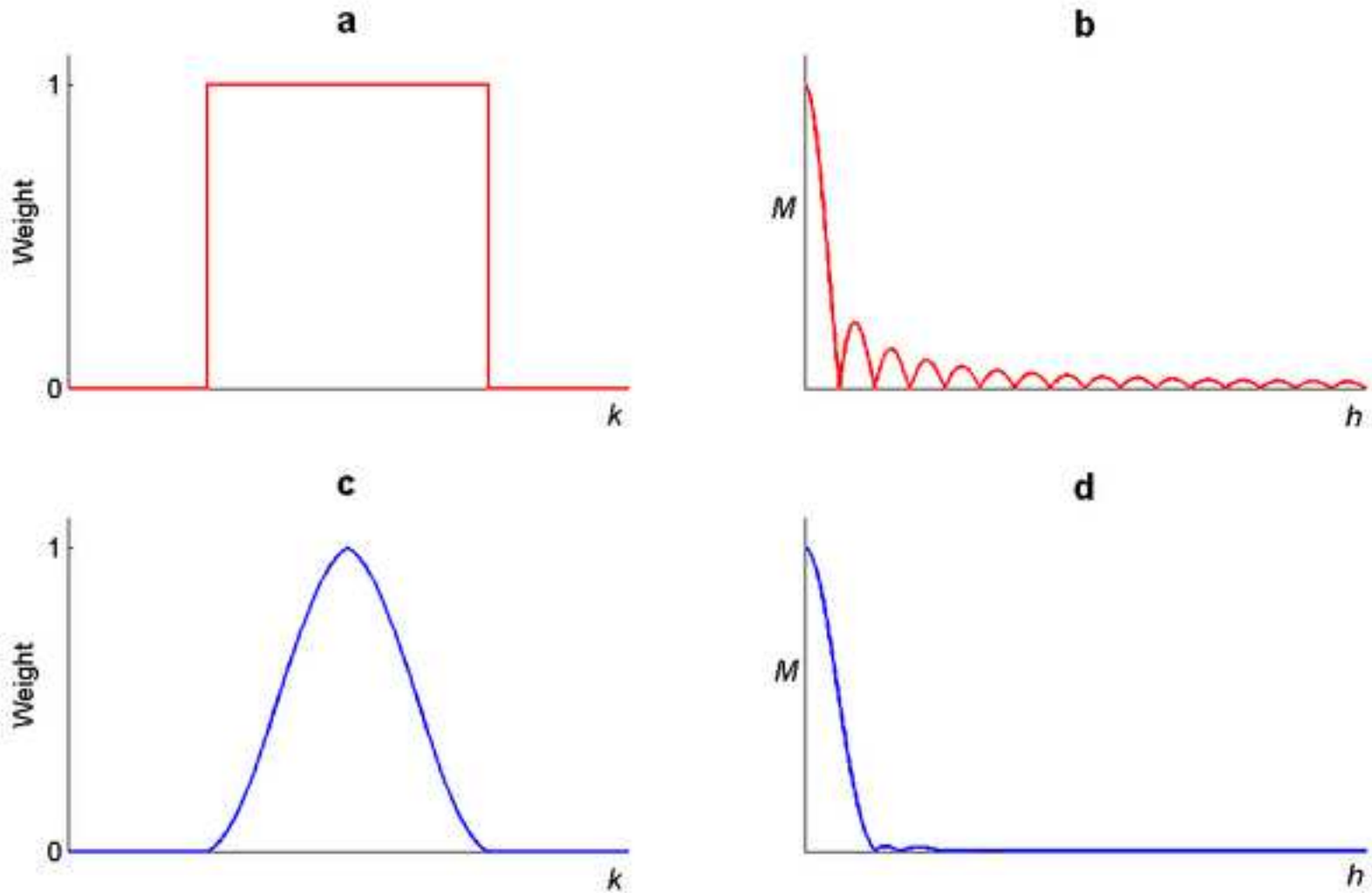

Figure

Click here to download Figure Figure_4.tif

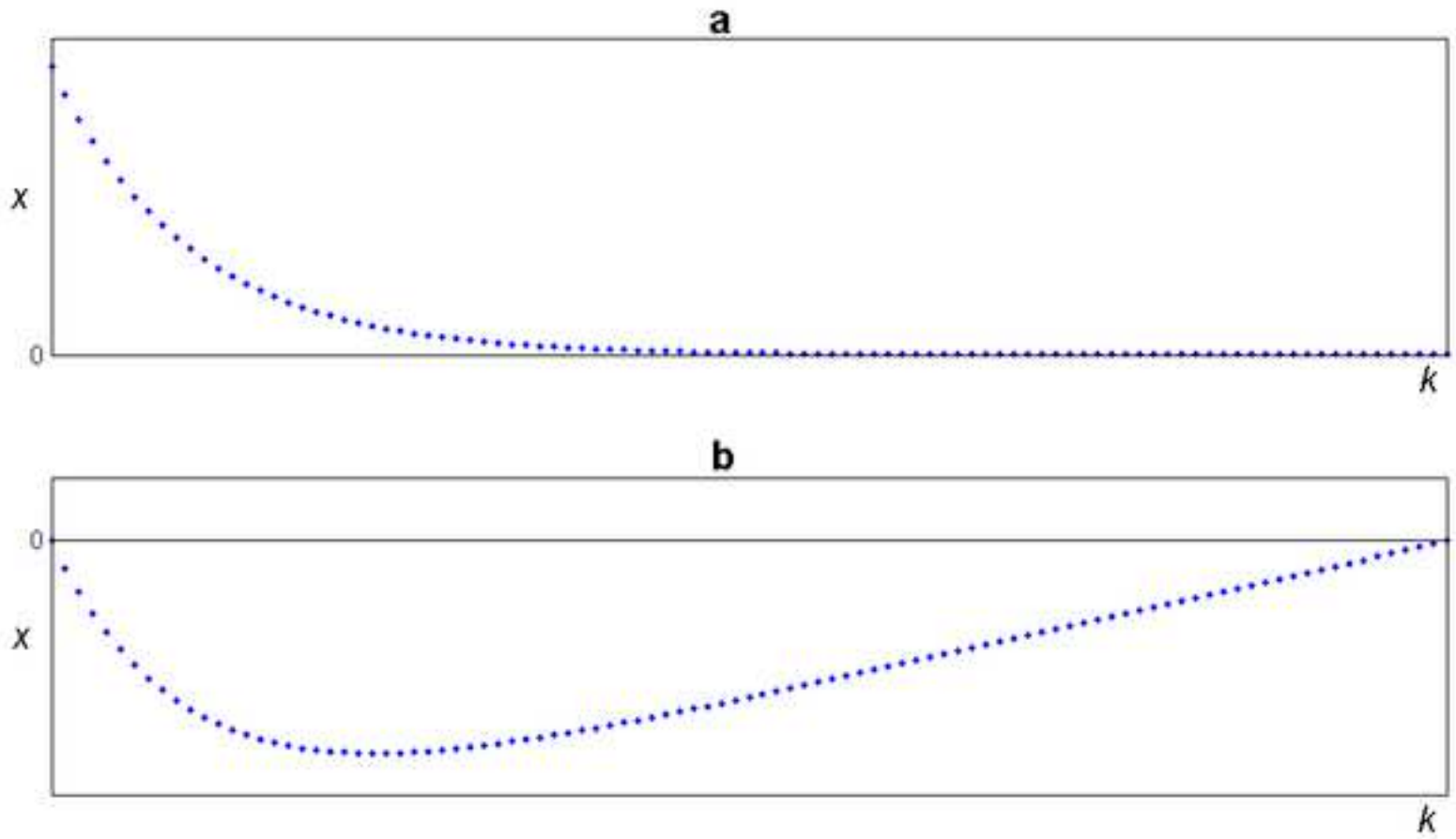

Figure

Click here to download Figure Figure_5.tif

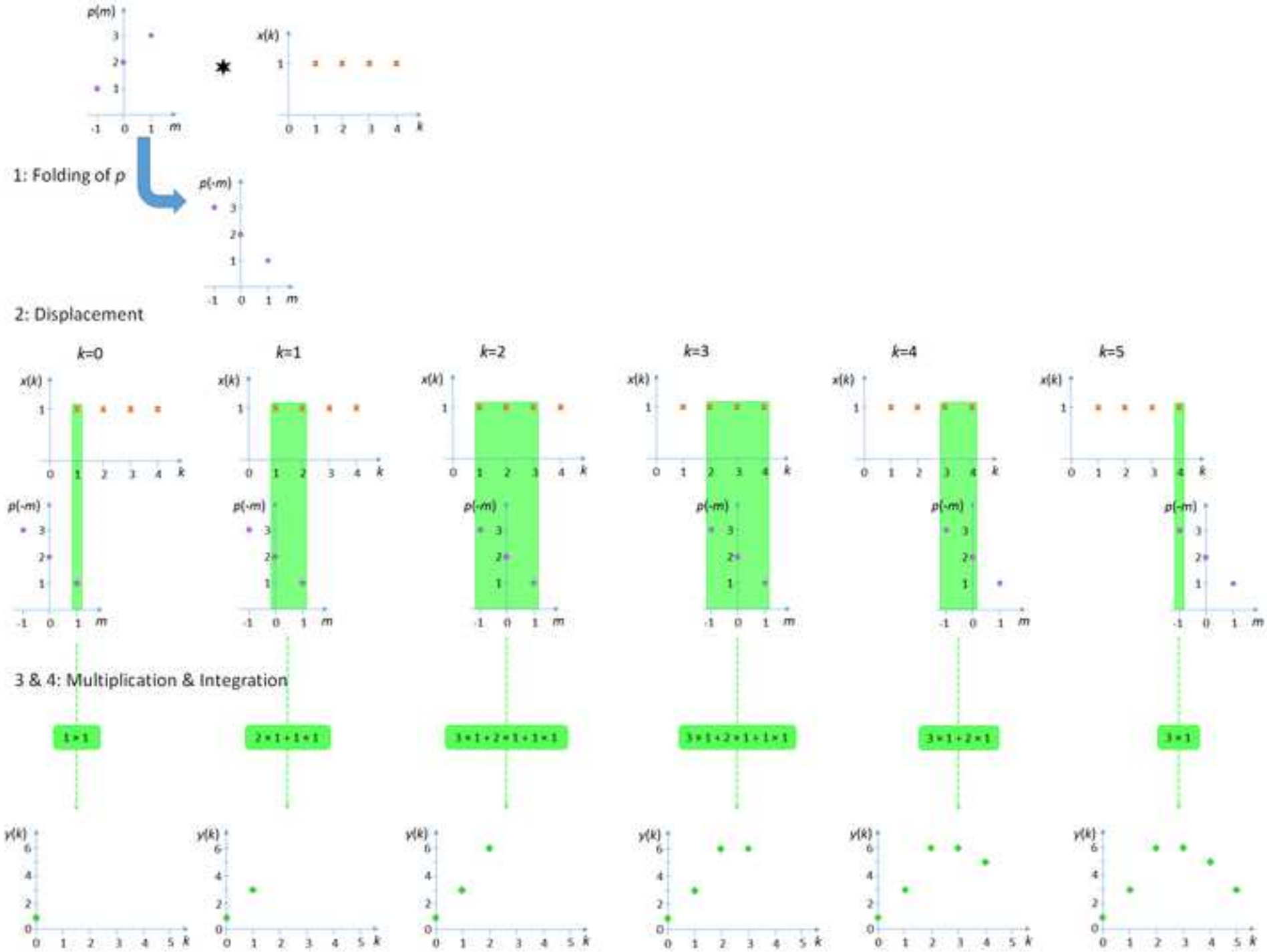

Click here to download Figure Figure_6.tif

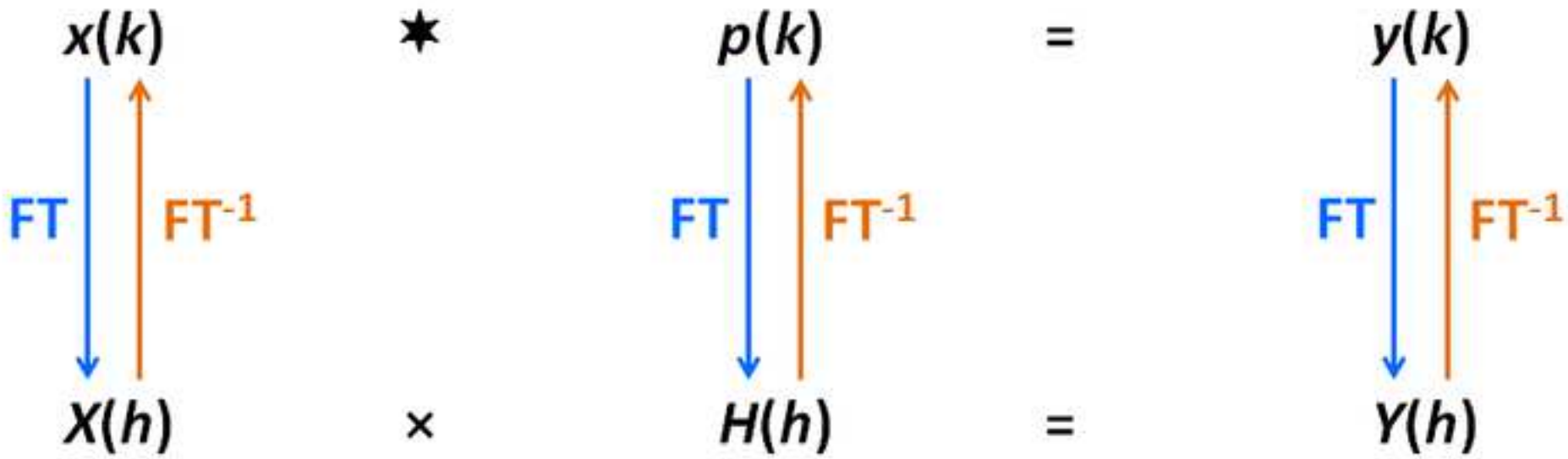

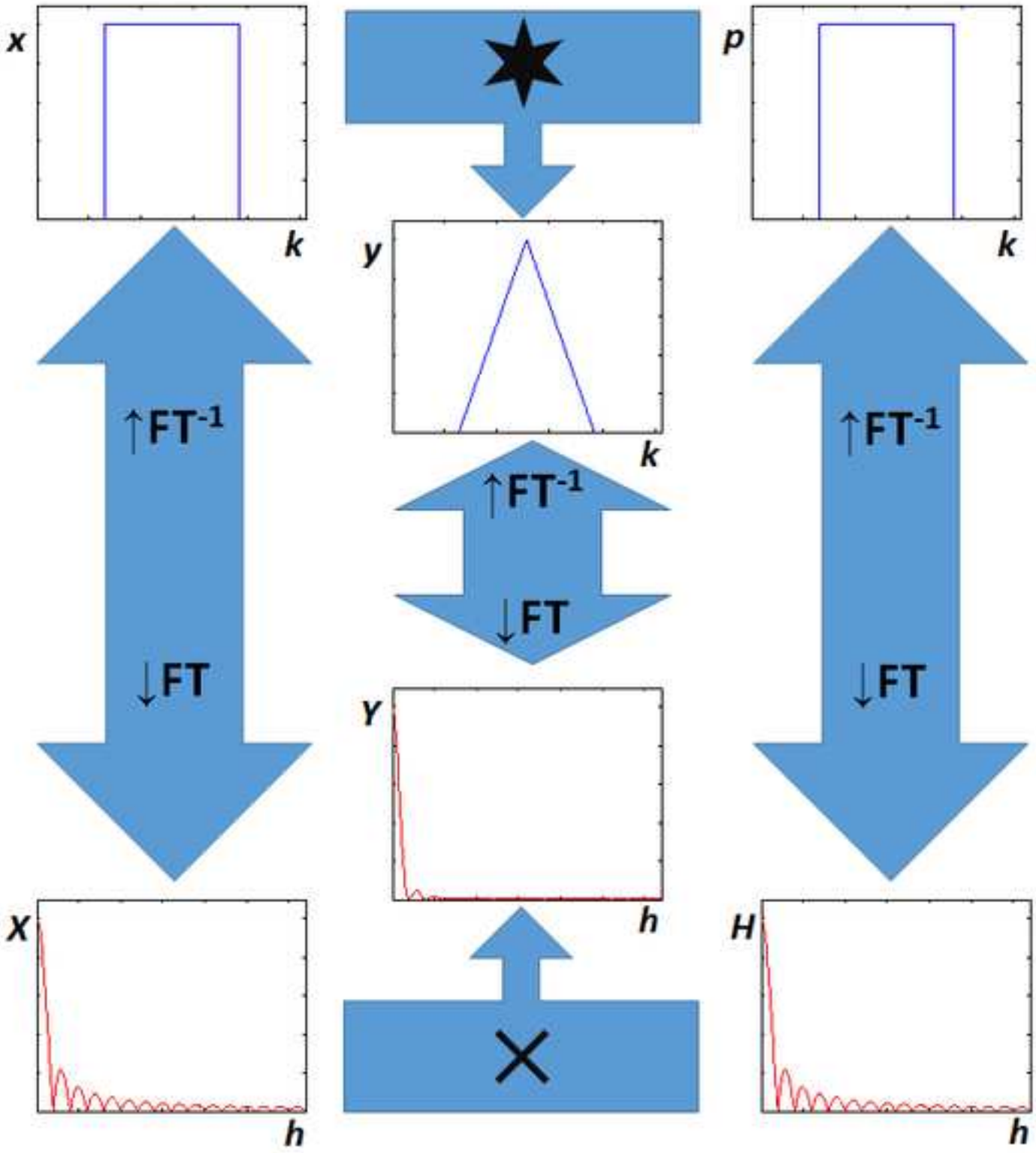
x
k
p
k
y
k
↑FT-1
↑FT-1
↓FT
↑FT-1
↓FT
Y
h
X
h
H
h

Click here to download Figure Figure_8.tif

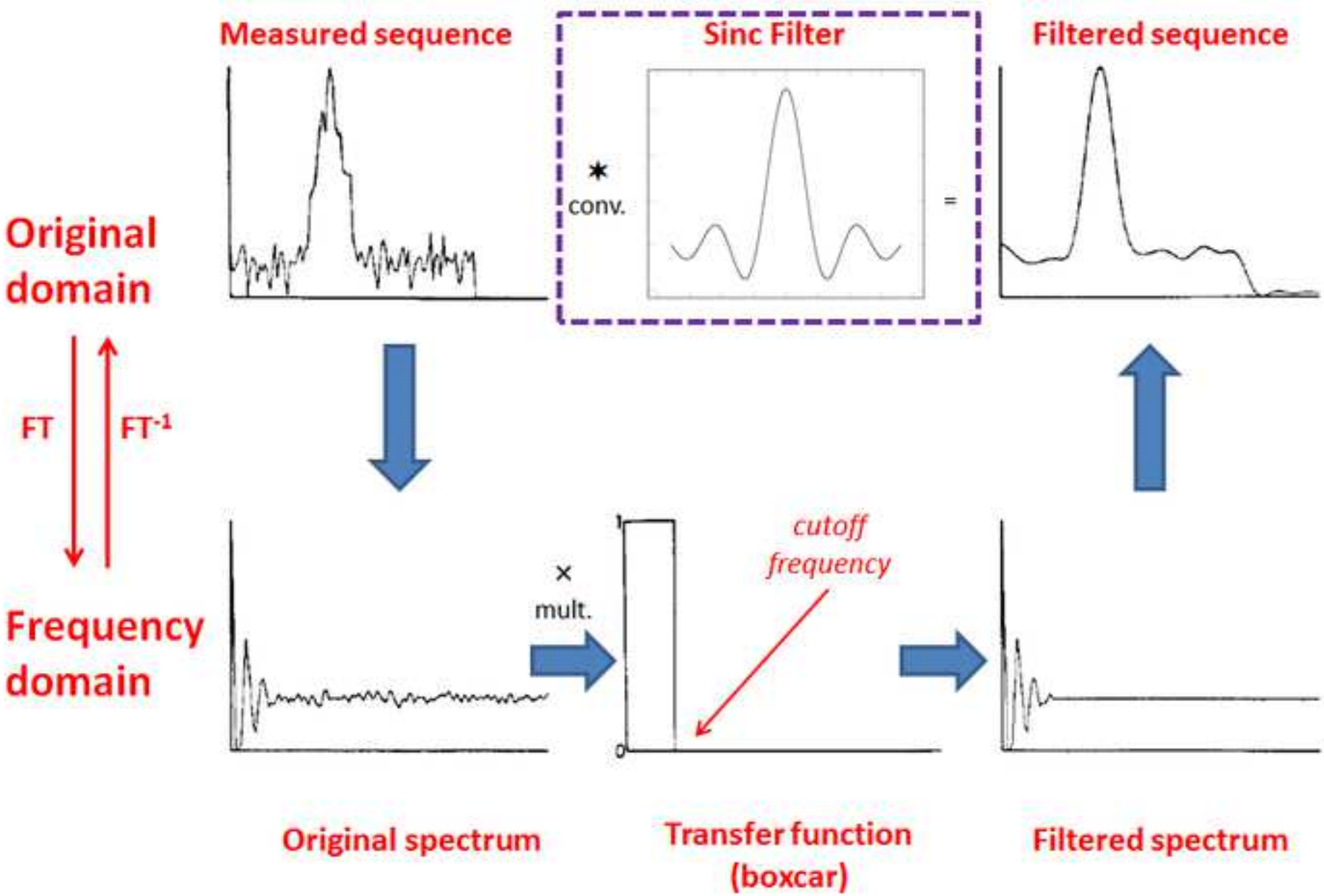

Click here to download Figure Figure_9.tif

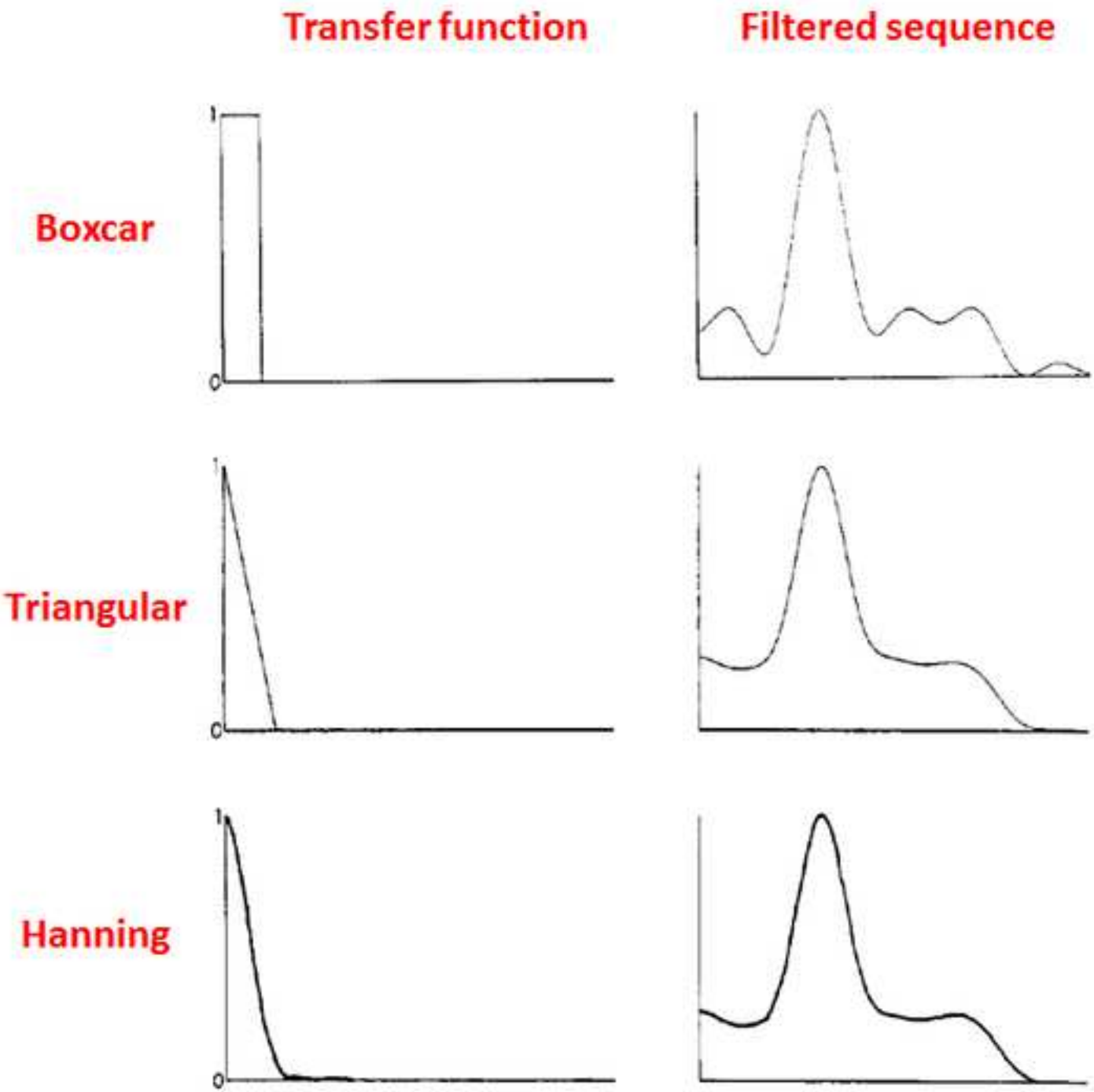

Click here to download Figure Figure_10.tif

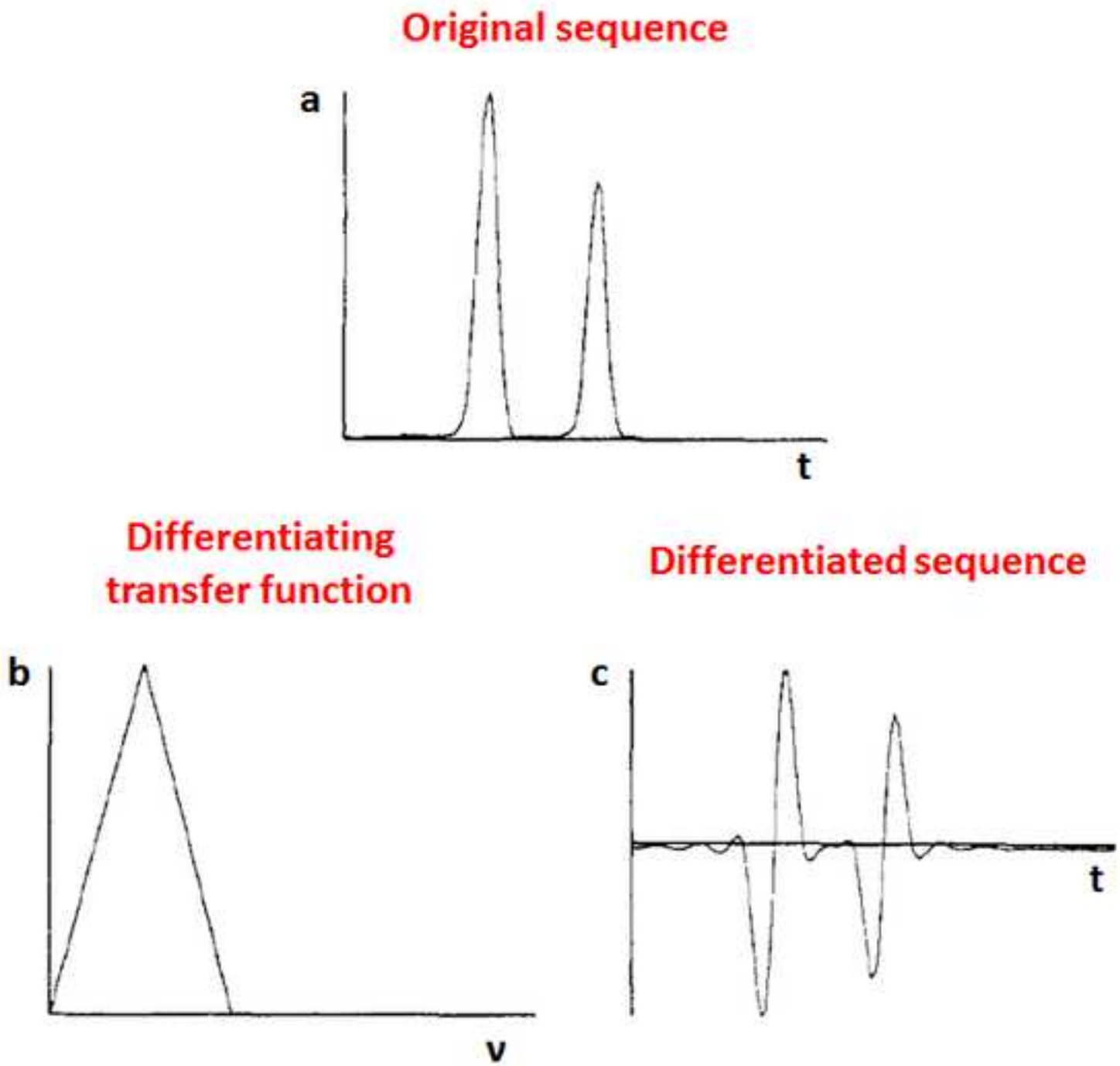

Figure

Click here to download Figure Figure_11.tif

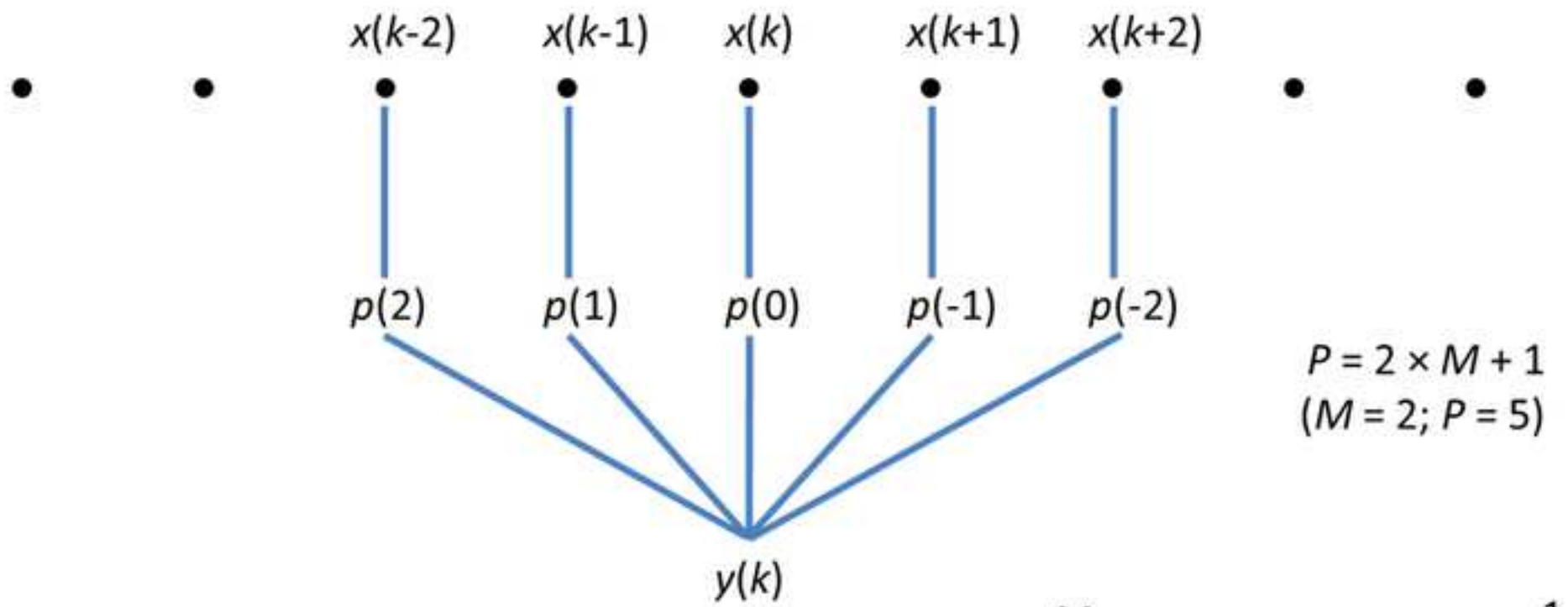

$P = 2 \times M + 1$

$(M = 2;\ P = 5)$

$$y(k) = \sum_{m=-M}^{M} [p(m) \times x(k-m)] \times \frac{1}{P}$$

Figure

Click here to download Figure Figure_12.tif

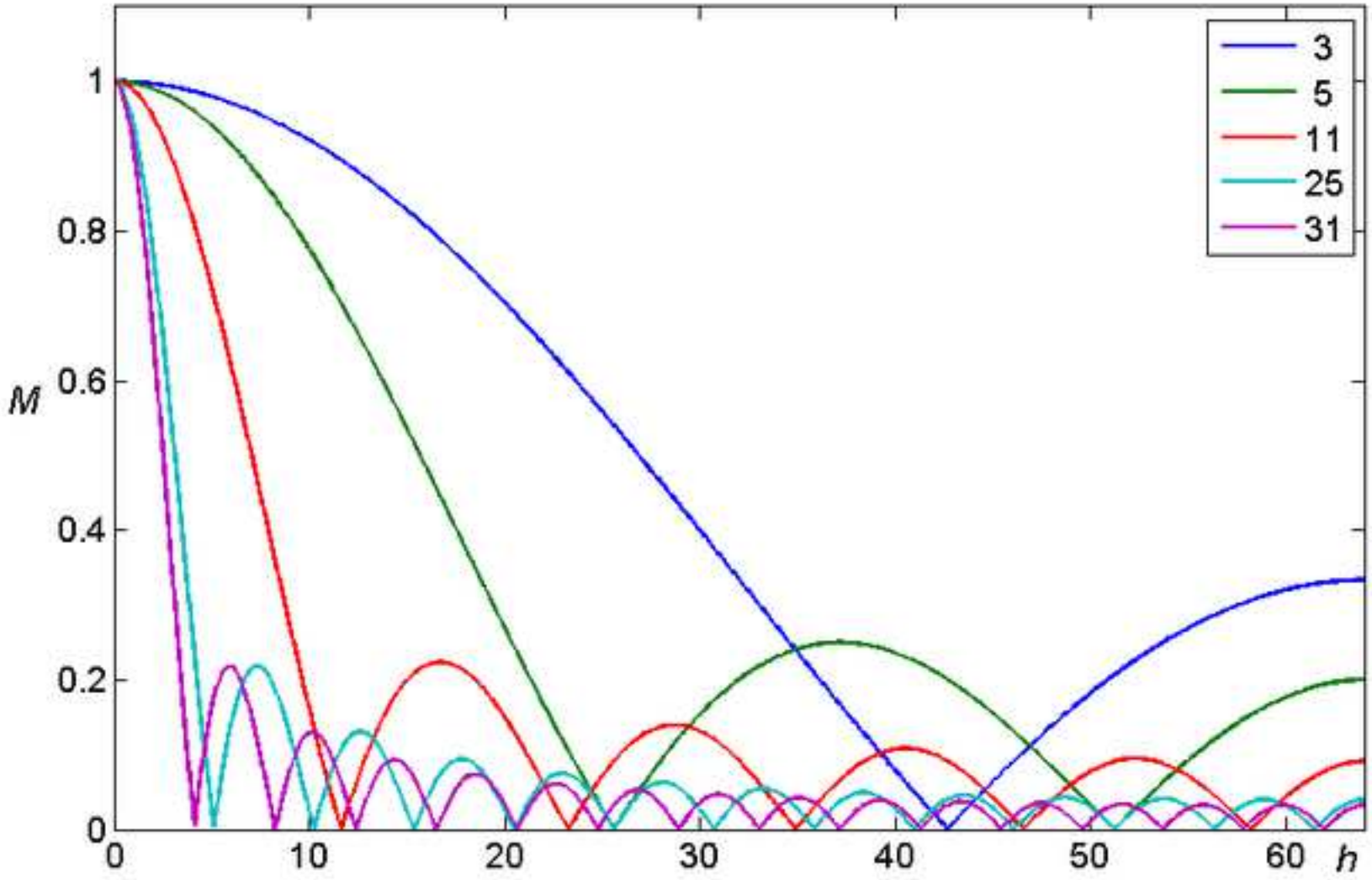

Figure

Click here to download Figure Figure_13.tif

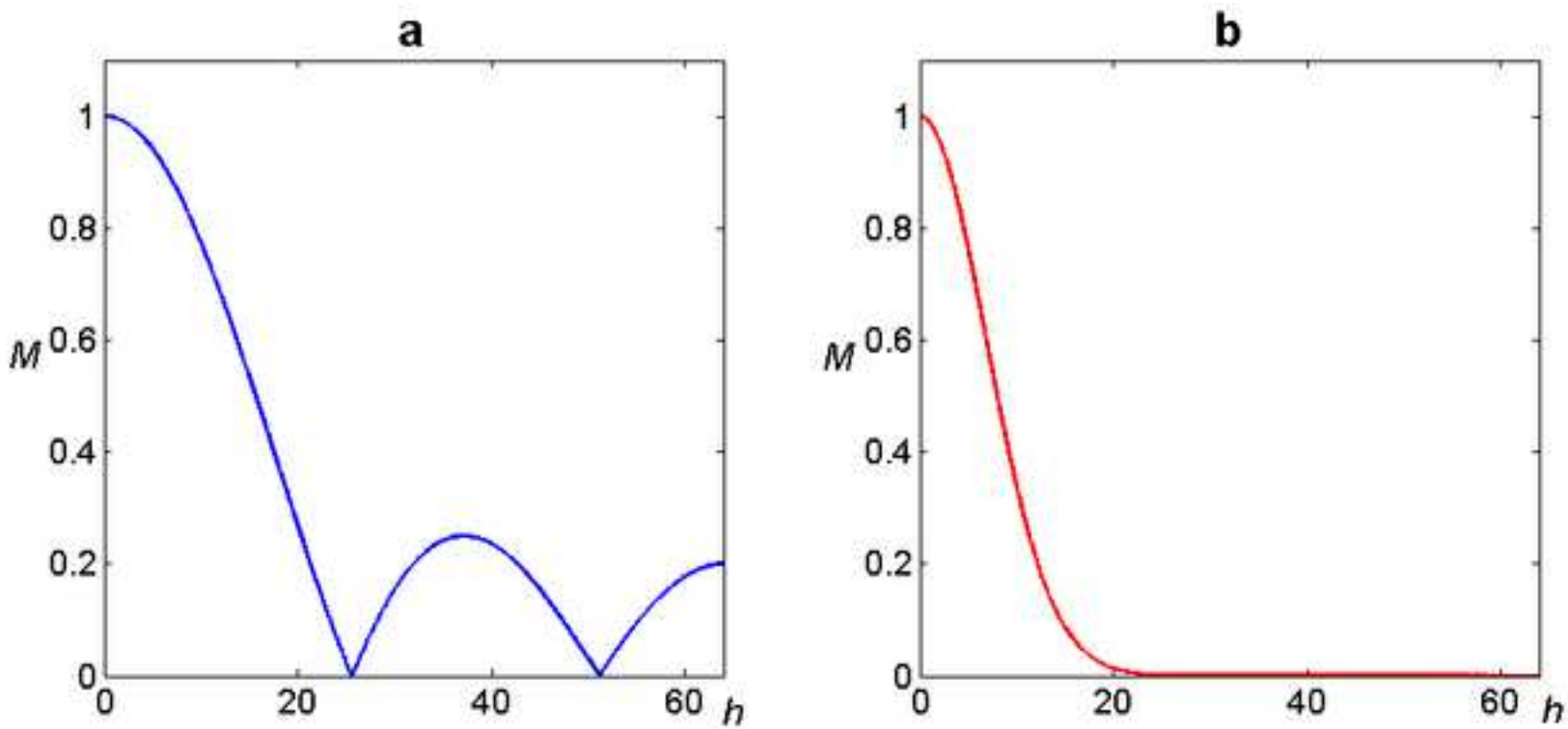

Figure

Click here to download Figure Figure_14.tif

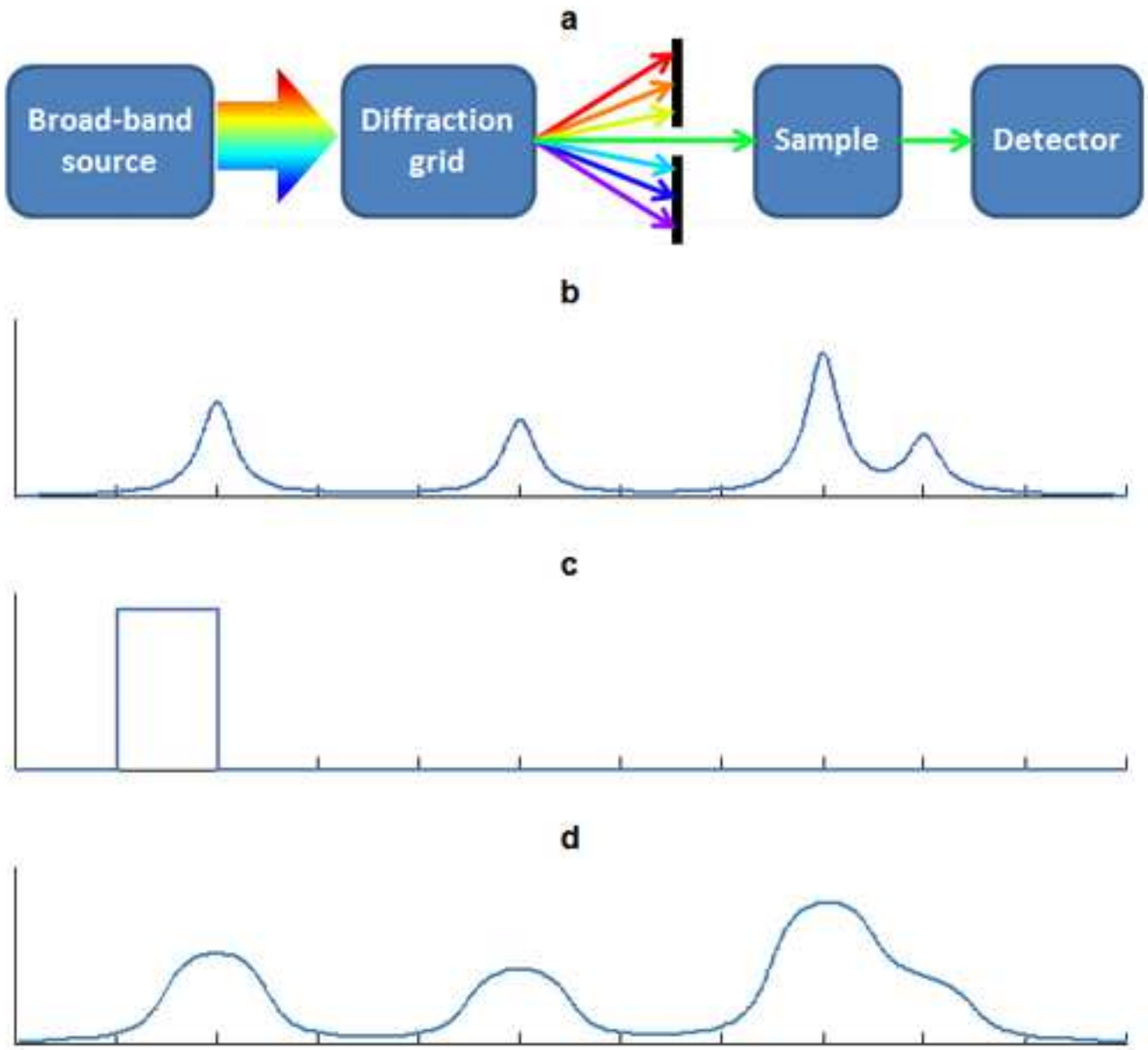

Figure

Click here to download Figure Figure_15.tif

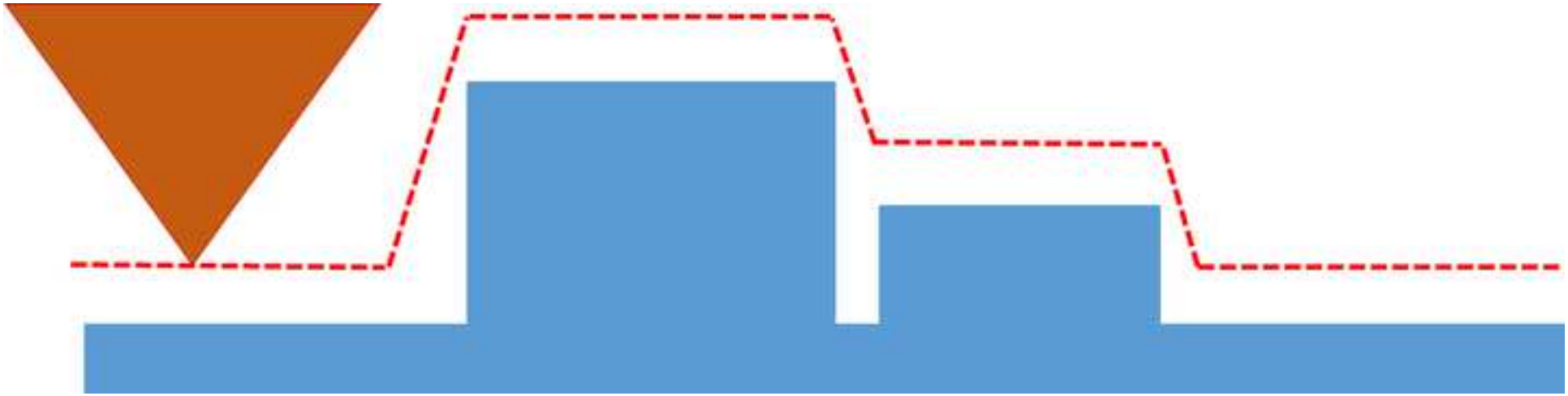

Figure

Click here to download Figure Figure_16.tif

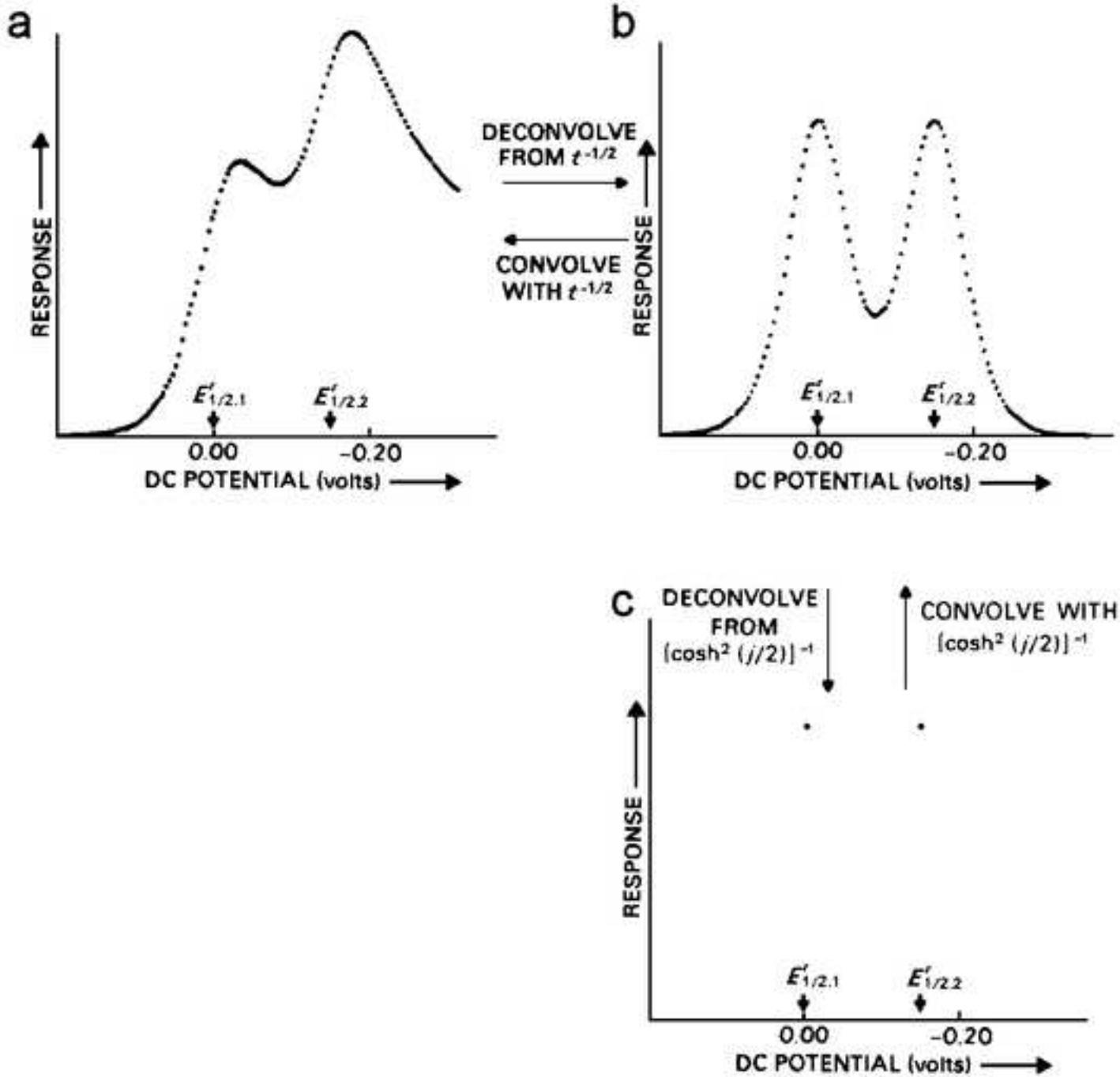

Figure

Click here to download Figure Figure_17.tif

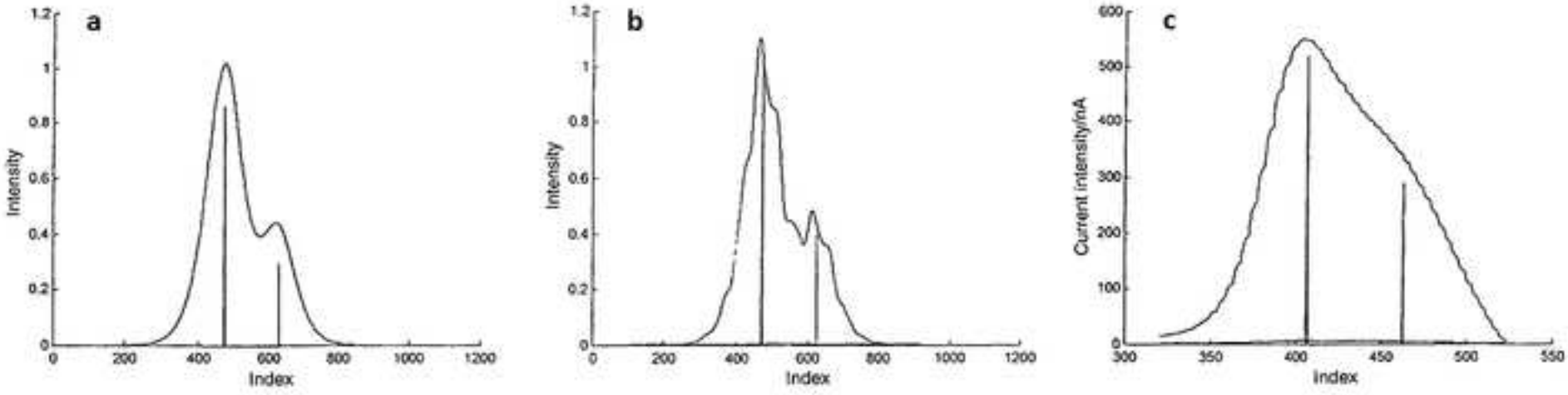

Figure

Click here to download Figure Figure_18.tif

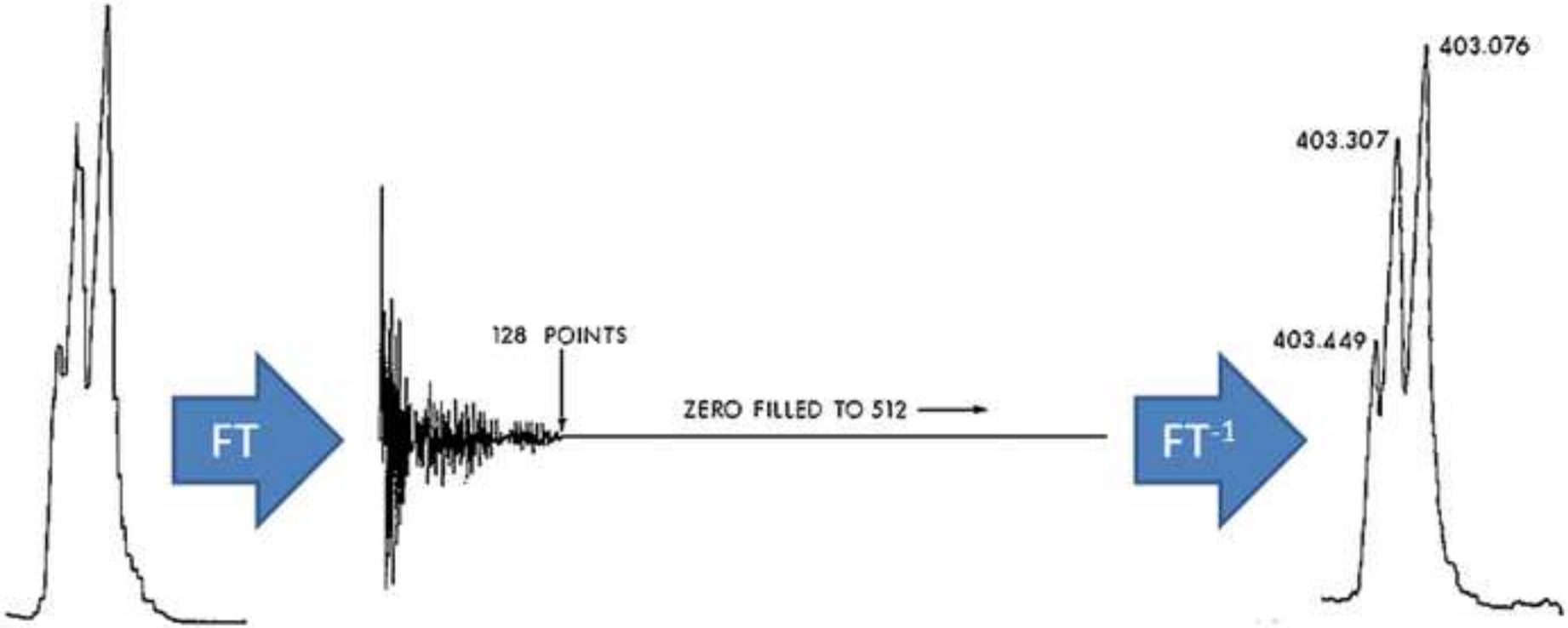

Click here to download Figure Figure_19.tif